$^{40}Ar/^{39}Ar$ METHODS

Following careful petrographical examination, samples were prepared as phenocryst-free groundmass separates (e.g., Mark et al., 2010) from aphyric rocks or as hornblende separates. Magnetic separation and thorough hand-picking ensured > 99% of phenocrysts were removed from the groundmass separates. Samples were packaged into Al-discs and irradiated for 5 minutes in the Cd-lined facility of the McMaster facility, Ontario, Canada. Alder Creek sanidine with an age of 1.193 ± 0.001 Ma (Nomade et al., 2005) was used as the fluence monitor for J-determinations. Samples were heated incrementally with a state-of-the-art, custom-built CO_2 laser system equipped with a digital Scanhead. The Scanhead allows for rapid rastering of the laser beam over large pits of mono-layer groundmass (up to 0.5g). The Gaussian profile of the CO_2 laser beam, which heats in a non-uniform manner, is modified by the scanning system to heat large sample quantities uniformly (see Wijbrans et al., 2011). Extracted gases were cleaned using two GP50 getters (one operated at 450 ˚C and one at room temperature) and a cold finger maintained at -140 ˚F. Data were collected using a fully automated MAP 215-50 mass spectrometer equipped with a Balzers SEV-217 electron multiplier. The mass spectrometer has a measured sensitivity of 1.13×10^{-13} moles/volt. Backgrounds were measured after every two analyses of unknowns. Average backgrounds ± standard deviation (n = 66, ^{40}Ar 1.02×10^{-15} moles, ^{39}Ar 3.10×10^{-17} moles, ^{38}Ar 1.90×10^{-17} moles, ^{37}Ar 7.85×10^{-17} moles, ^{36}Ar 1.38×10^{-17} moles) from the entire run sequence were used to correct raw isotope measurements of unknowns. Mass discrimination was monitored by analysis of air pipettes after every five analyses (average ± standard deviation, n = 21, $^{40}Ar/^{36}Ar$ = 288.3 ± 0.6). Isotope data were corrected for blanks, radioactive decay, mass discrimination and interfering reactions using the approach of Mark et al., (2011). The decay constants of Steiger and Jäger (1977) were used and ages are quoted at the 1σ confidence level. Raw isotope data and both age spectra and isotope correlation plots can be found in GSA Date Repository. The criteria for fitting of plateaus was they must include at least 60% of ^{39}Ar in three or more contiguous steps with the probability of fit of plateau to data >0.05. Note plateaus also define inverse isochrons on isotope correlation plots with y-axis intercepts ($^{36}Ar/^{40}Ar$) that overlap with the accepted air Ar isotope ratios (Nier, 1950).

REFERENCES CITED

Mark, D.F., Gonzales, S., Huddart, D., and Bohnel, H., 2010, Dating of the Valsequillo volcanic deposits: Resolution of an ongoing controversy in Central Mexico: Journal of Human Evolution, v. 58, p. 441-445.

Mark, D.F., Rice, C.M., Fallick, A.E., Trewin, N.H., Lee, M.R., Boyce, A., and Lee, J.K.W., 2011, Ar/Ar dating of hydrothermal activity, biota and gold mineralization in the Rhynie hot-spring system, Aberdeenshire, Scotland.: Geochimica et Cosmochimica Acta, v. 75, p. 555-569.

Nier, A.O., 1950, A redetermination of the relative abundances of the isotopes of carbon, nitrogen, oxygen, argon and potassium.: Physical Reviews, v. 77, p. 789-793.

Nomade, S., Renne, P.R., Vogel, N., Deino, A.L., Sharp, W.D., Becker, T.A., Jaouni, A.R., and Mundil, R., 2005, Alder Creek sanidine (ACs-2): a Quaternary $^{40}Ar^{39}/Ar$ dating standard tied to the Cobb Mountain geomagnetic event: Chemical Geology, v. 218, p. 315-338.

Steiger, R.H., and Jäger, E., 1977, Subcommission on geochronology: convention on the use of decay constants in geo- and cosmochronology.: Earth & Planetary Science Letters, v. 6, p. 359-362.

Wijbrans, J., Schneider, B., Kuiper, K., Calvari, S., Branca, S., De Beni, E., Norini, G., Corsaro, R.A., and Miraglia, L., 2011, $^{40}Ar/^{39}Ar$ geochronology of Holocene basalts; examples from Stromboli, Italy: Quaternary Geochronology, v. 6, p. 223-232.

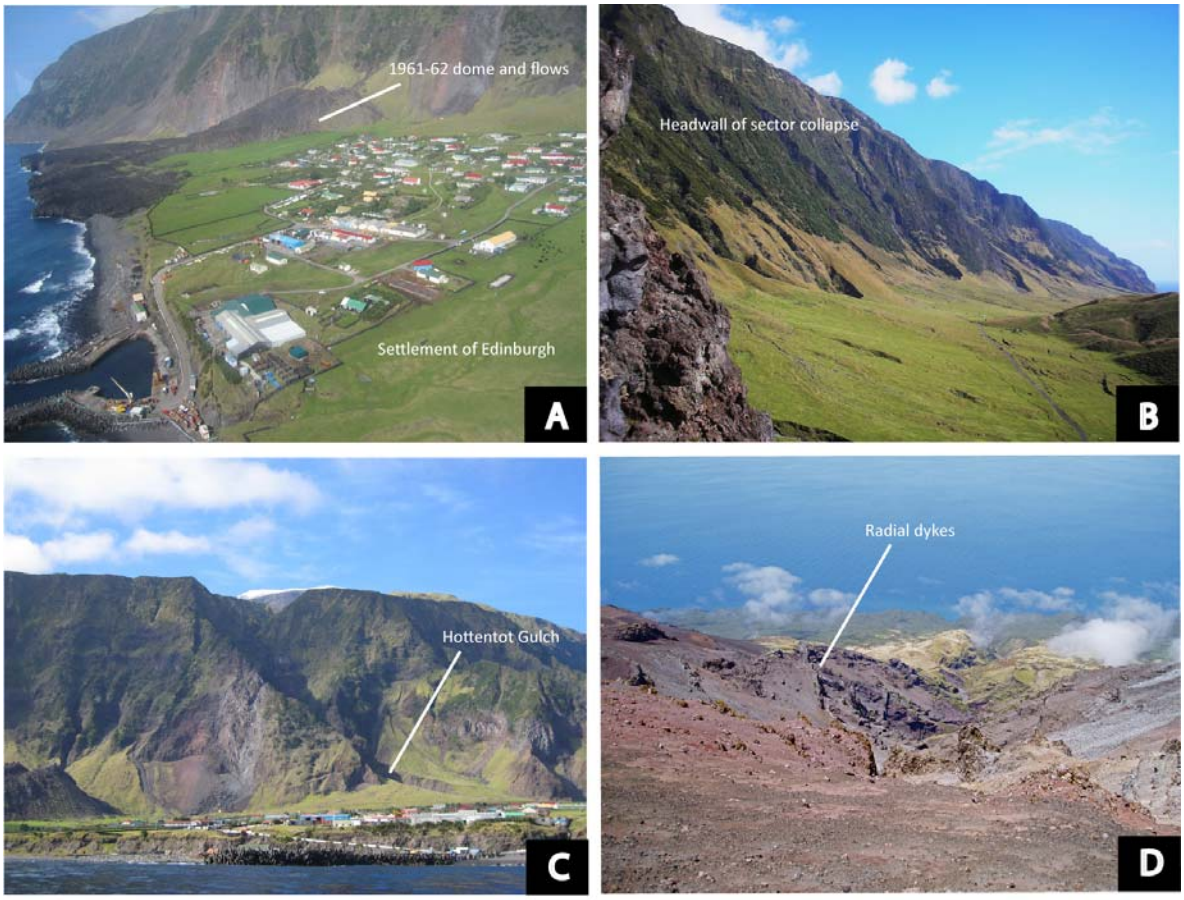

Fig. DB1. Morphological features on Tristan da Cunha. A: Image showing the proximity of the Settlement to the 1961-62 dome and flows (photo courtesy of Vicky Hards). B: Headwall of the sector collapse scar on the north-western coastal strip. The single road leading from the Settlement to the Potato Patches can be seen and the position of the Hillpiece-Burnthill complex is visible to the right of the frame. C: View to the South showing sheer cliffs (sector collapse headwall) with the position of one of the main gulches (canyons) (photo courtesy of Vicky Hards). D: View from the summit showing radial dykes.

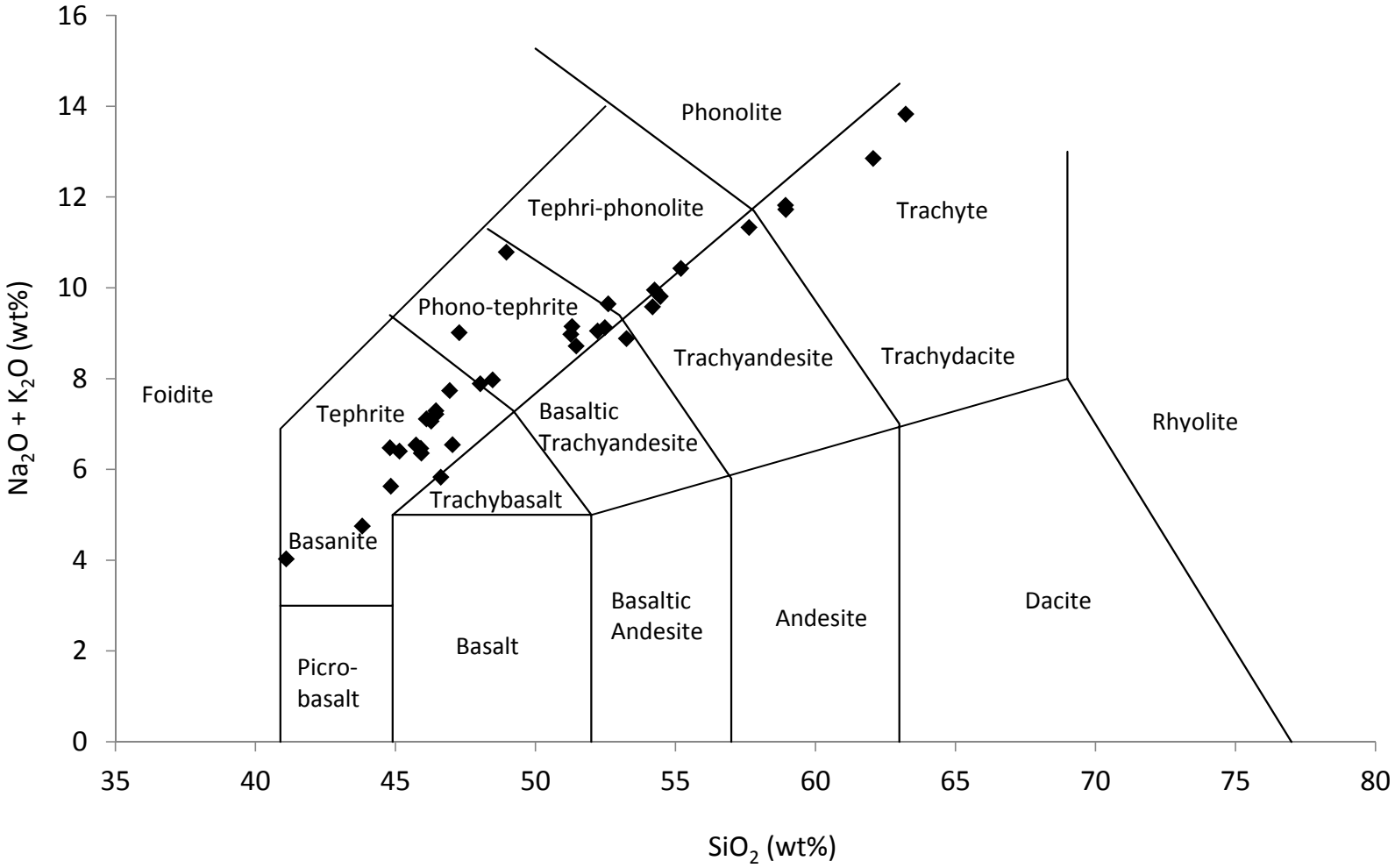

Fig. DR2. TAS diagram for 35 analyzed samples from Tristan da Cunha

TDCAH007 Age spectra and inverse isochrons of fifteen volcanic samples from Tristan da Cunha. Both the plateau and inverse isochron ages are within error of each other, indicating that the 40Ar/39Ar ages are robust.

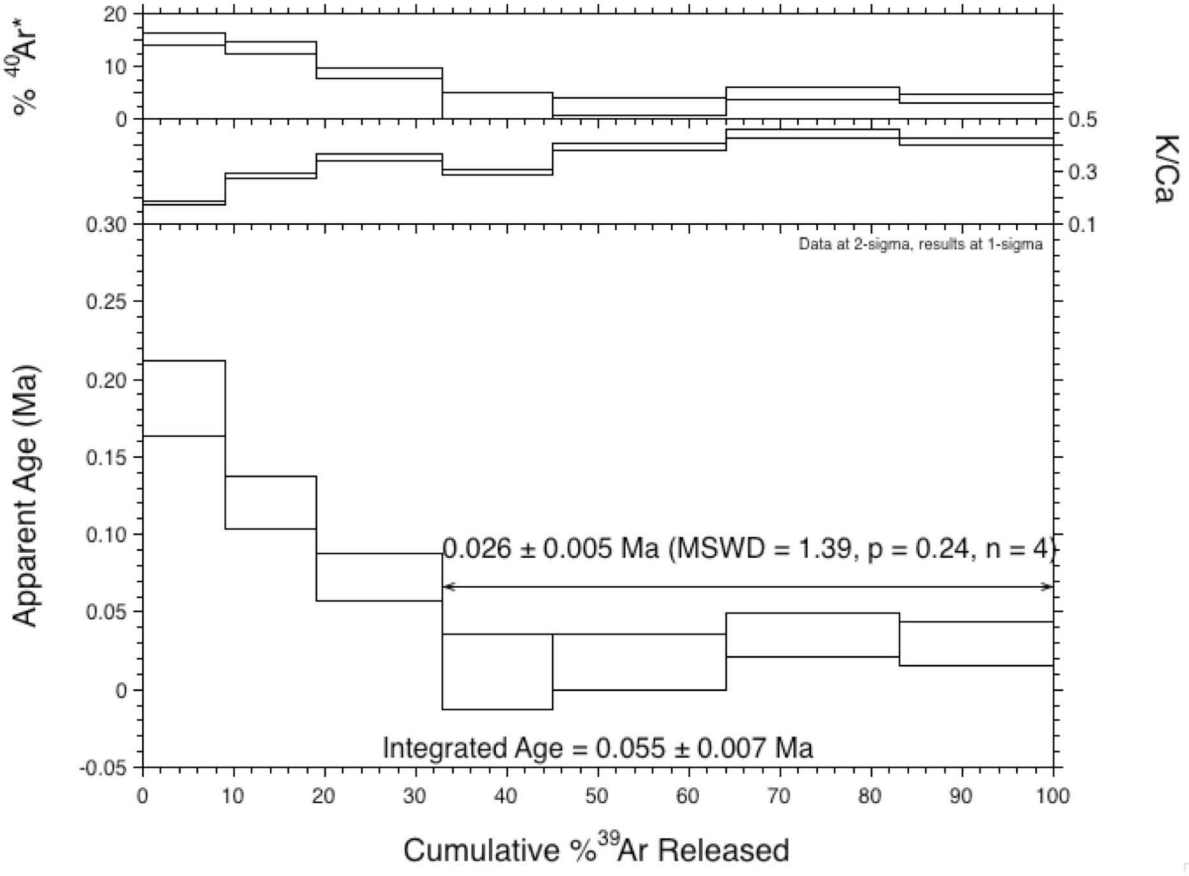

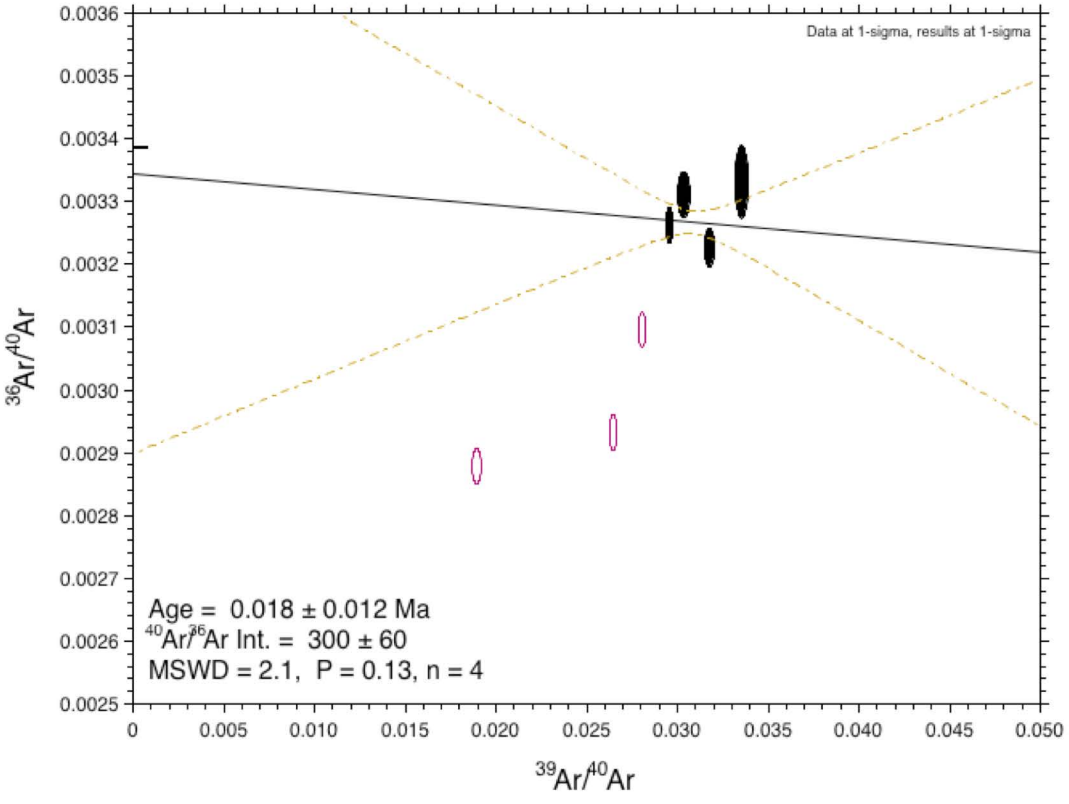

TDCAH052

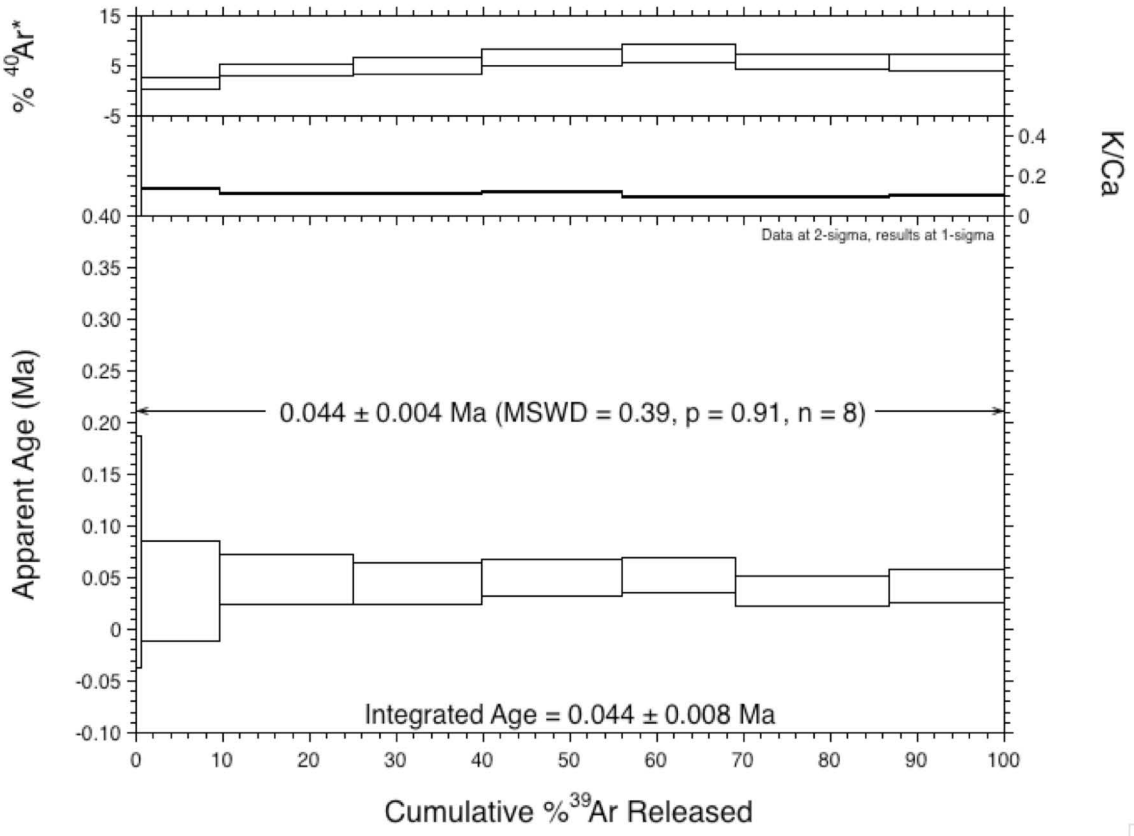
% 40Ar*
K/Ca
Data at 2-sigma, results at 1-sigma
Apparent Age (Ma)
0.044 ± 0.004 Ma (MSWD = 0.39, p = 0.91, n = 8)
Integrated Age = 0.044 ± 0.008 Ma
Cumulative %39Ar Released

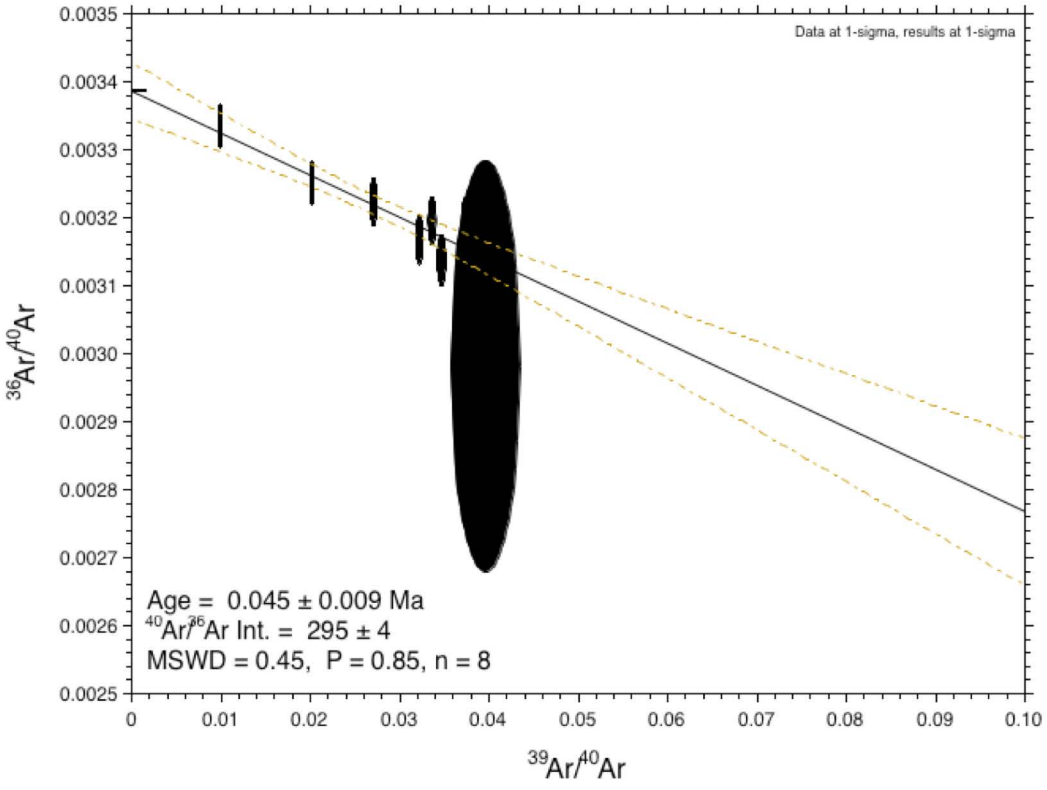
Data at 1-sigma, results at 1-sigma
36Ar/40Ar
Age = 0.045 ± 0.009 Ma
40Ar/36Ar Int. = 295 ± 4
MSWD = 0.45, P = 0.85, n = 8
39Ar/40Ar

TDCAH054

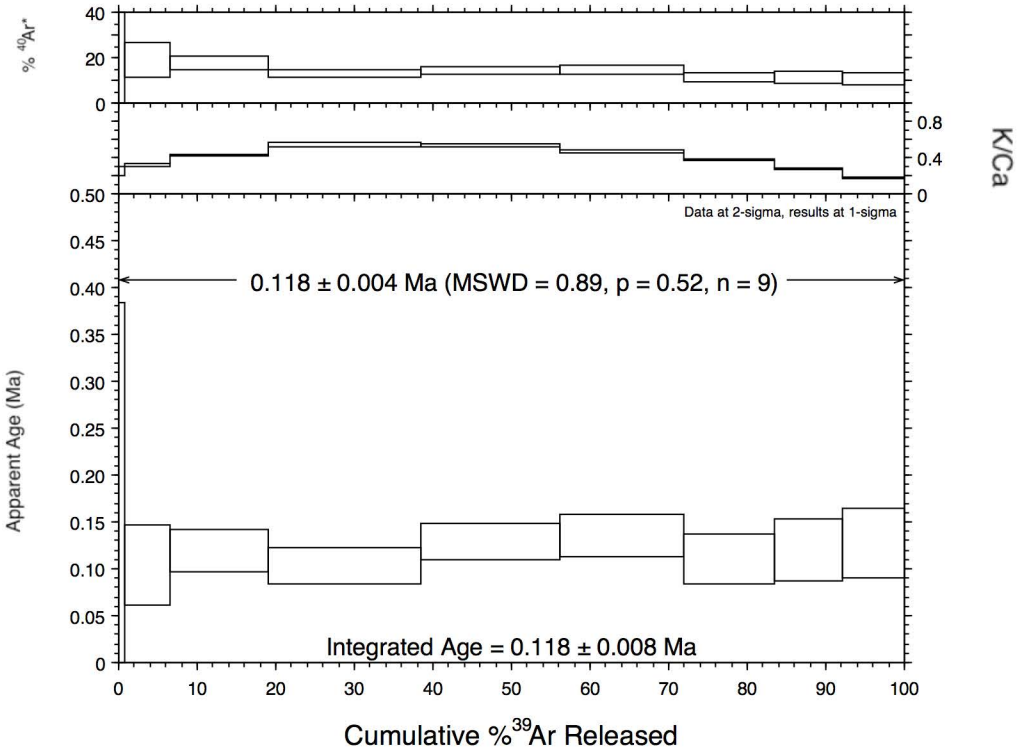
% 40Ar*
K/Ca
Data at 2-sigma, results at 1-sigma
0.118 ± 0.004 Ma (MSWD = 0.89, p = 0.52, n = 9)
Apparent Age (Ma)
Integrated Age = 0.118 ± 0.008 Ma
Cumulative %39Ar Released

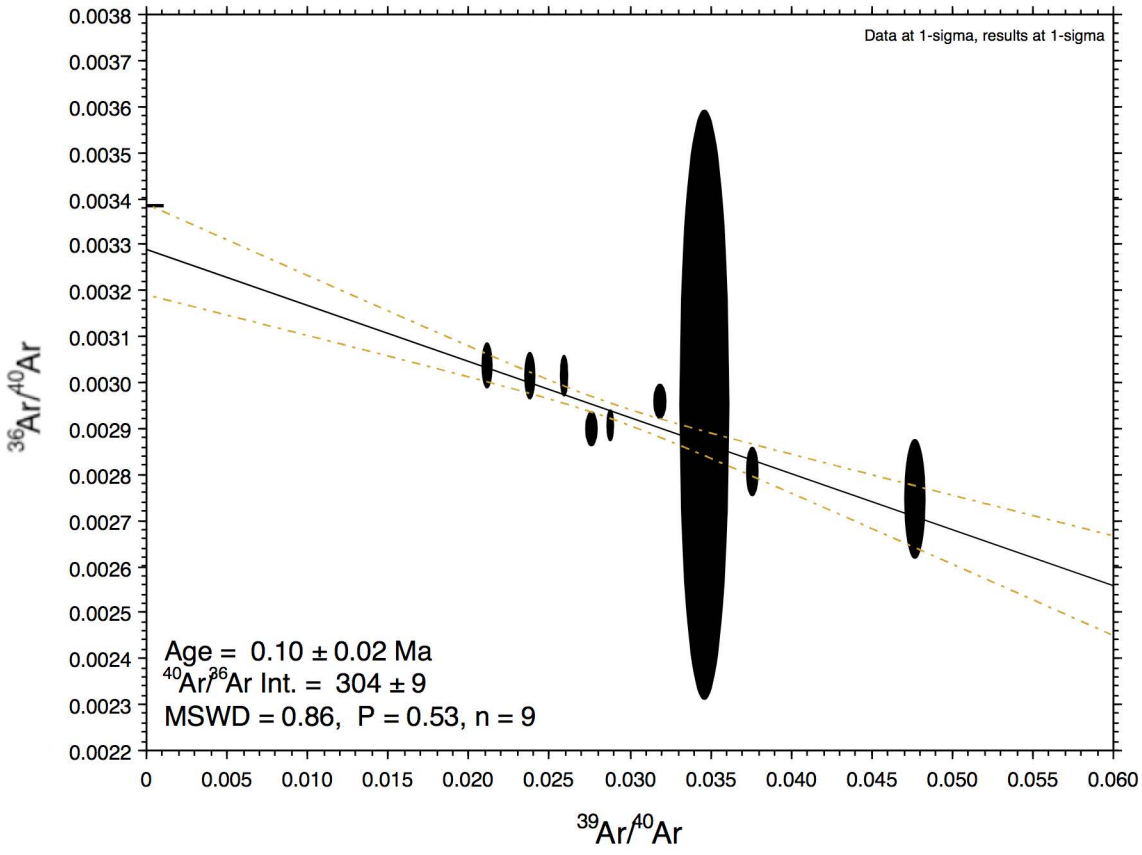
Data at 1-sigma, results at 1-sigma
Age = 0.10 ± 0.02 Ma
40Ar/36Ar Int. = 304 ± 9
MSWD = 0.86, P = 0.53, n = 9
36Ar/40Ar
39Ar/40Ar

TDCAH085

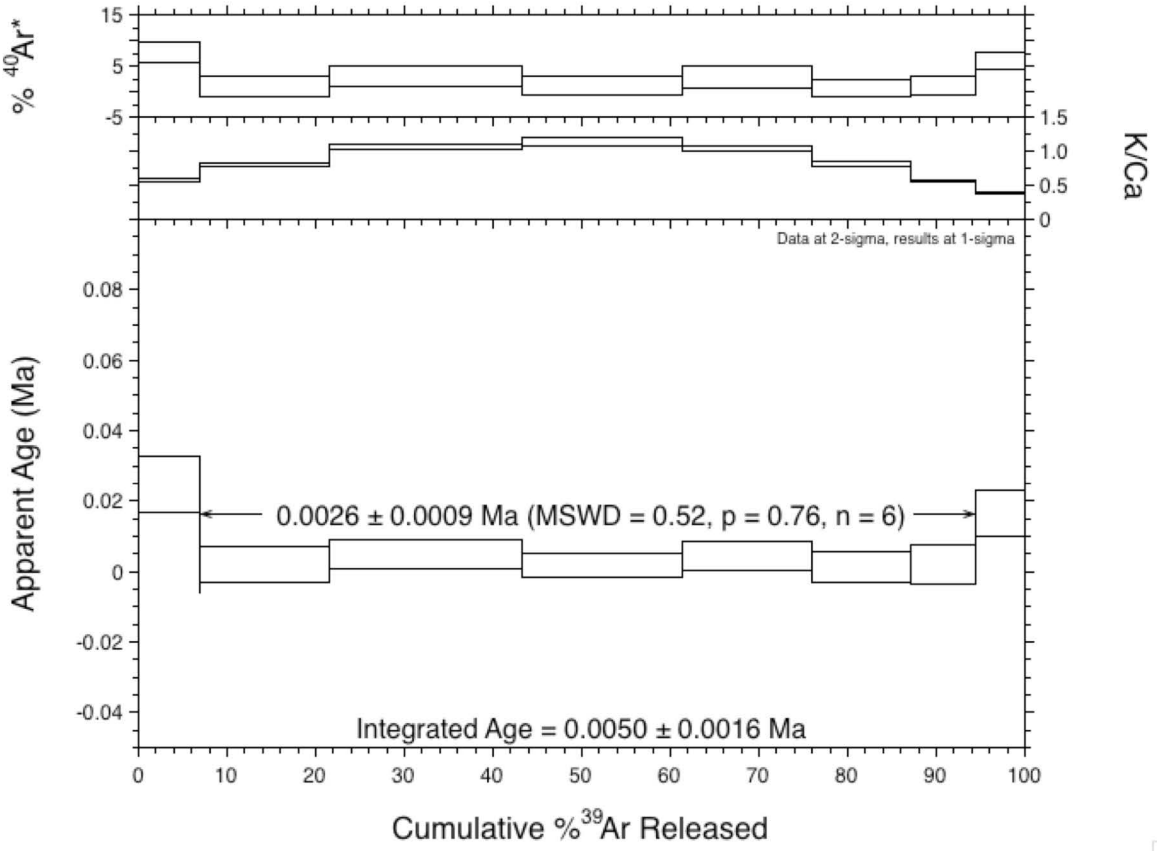
% 40Ar*
15
5
-5
K/Ca
1.5
1.0
0.5
0
Data at 2-sigma, results at 1-sigma
Apparent Age (Ma)
0.08
0.06
0.04
0.02
0
-0.02
-0.04
0.0026 ± 0.0009 Ma (MSWD = 0.52, p = 0.76, n = 6)
Integrated Age = 0.0050 ± 0.0016 Ma
0
10
20
30
40
50
60
70
80
90
100
Cumulative %39Ar Released

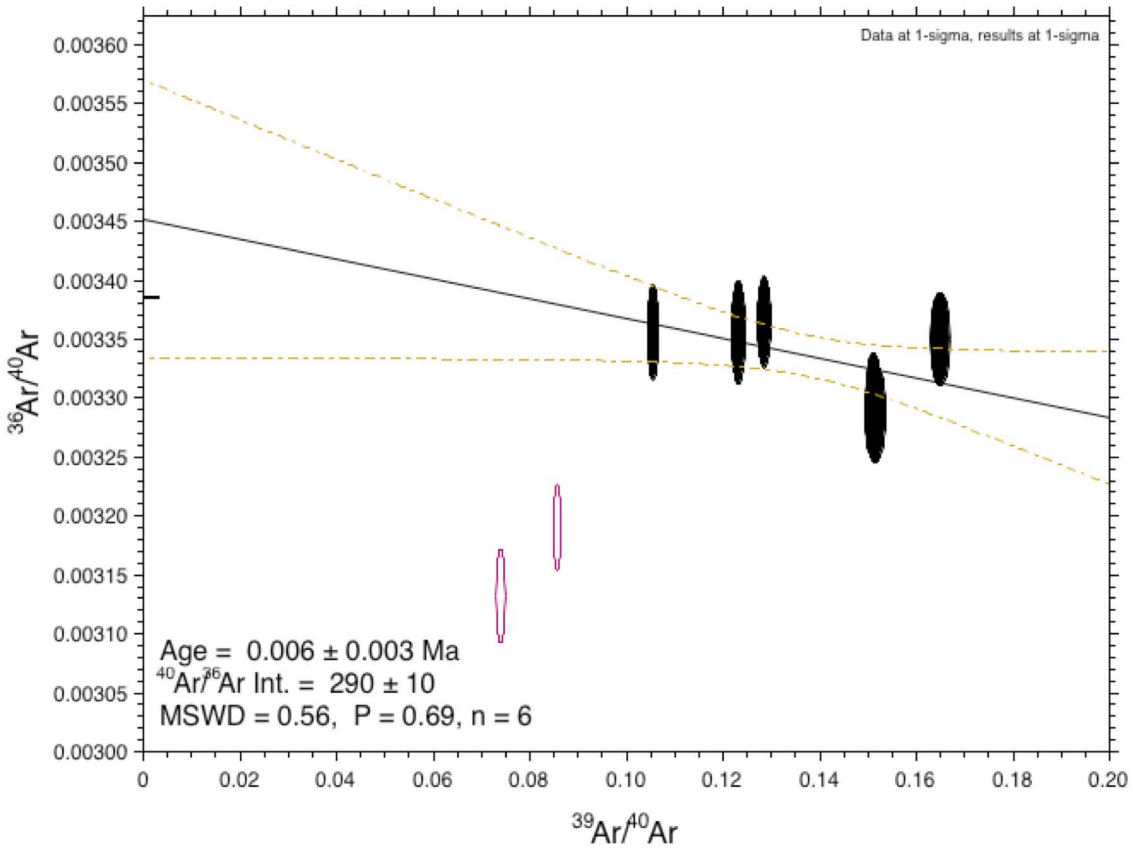
Data at 1-sigma, results at 1-sigma
36Ar/40Ar
0.00360
0.00355
0.00350
0.00345
0.00340
0.00335
0.00330
0.00325
0.00320
0.00315
0.00310
0.00305
0.00300
Age = 0.006 ± 0.003 Ma
40Ar/36Ar Int. = 290 ± 10
MSWD = 0.56, P = 0.69, n = 6
0
0.02
0.04
0.06
0.08
0.10
0.12
0.14
0.16
0.18
0.20
39Ar/40Ar

TDCAH089

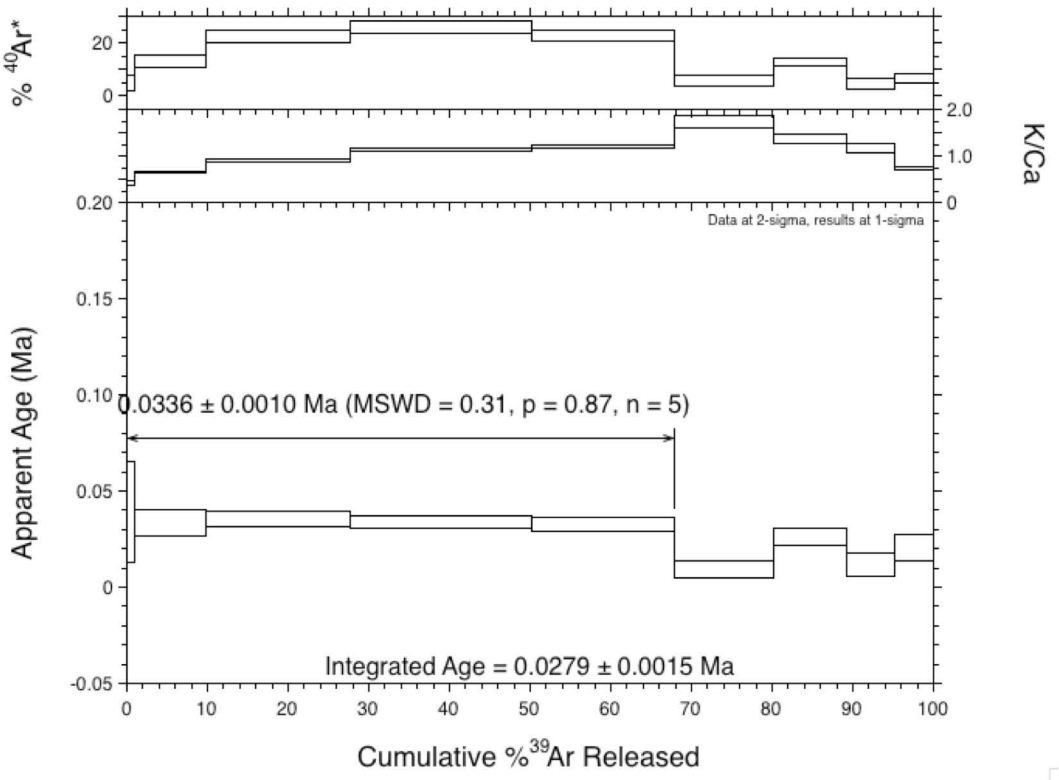
% 40Ar*
K/Ca
Data at 2-sigma, results at 1-sigma
Apparent Age (Ma)
0.0336 ± 0.0010 Ma (MSWD = 0.31, p = 0.87, n = 5)
Integrated Age = 0.0279 ± 0.0015 Ma
Cumulative %39Ar Released

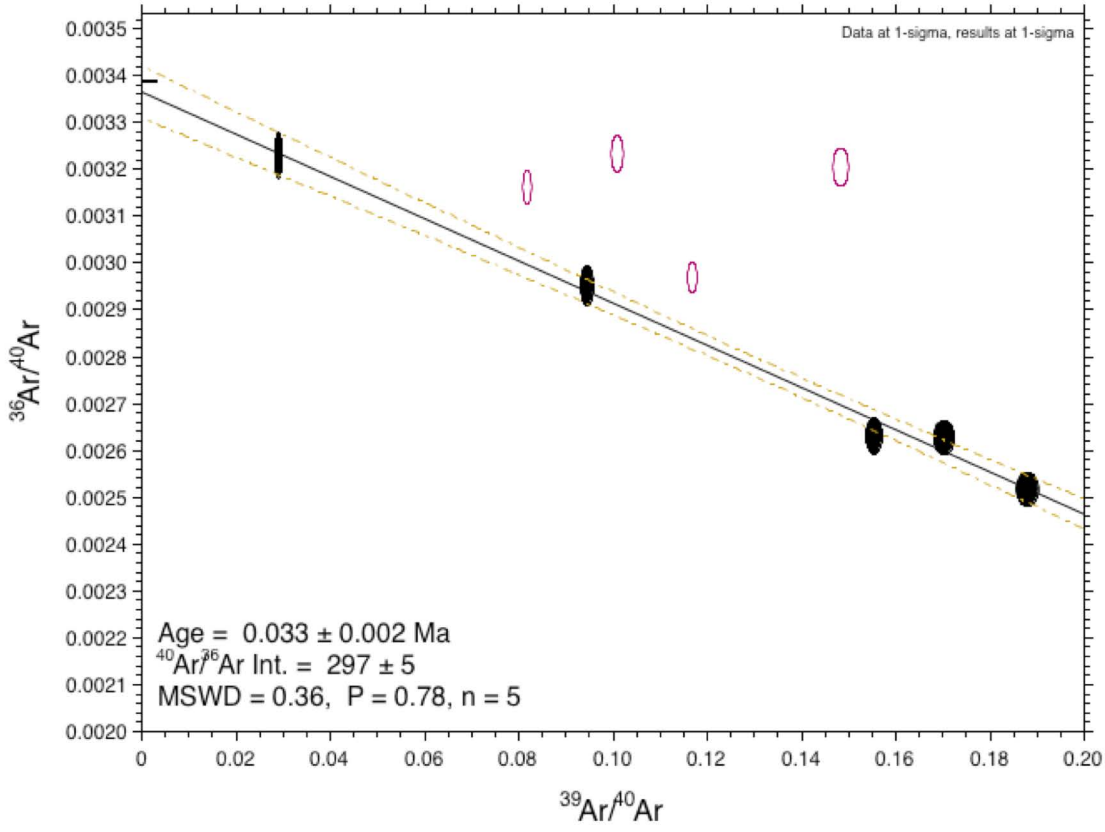
Data at 1-sigma, results at 1-sigma
36Ar/40Ar
Age = 0.033 ± 0.002 Ma
40Ar/36Ar Int. = 297 ± 5
MSWD = 0.36, P = 0.78, n = 5
39Ar/40Ar

TDCAH093

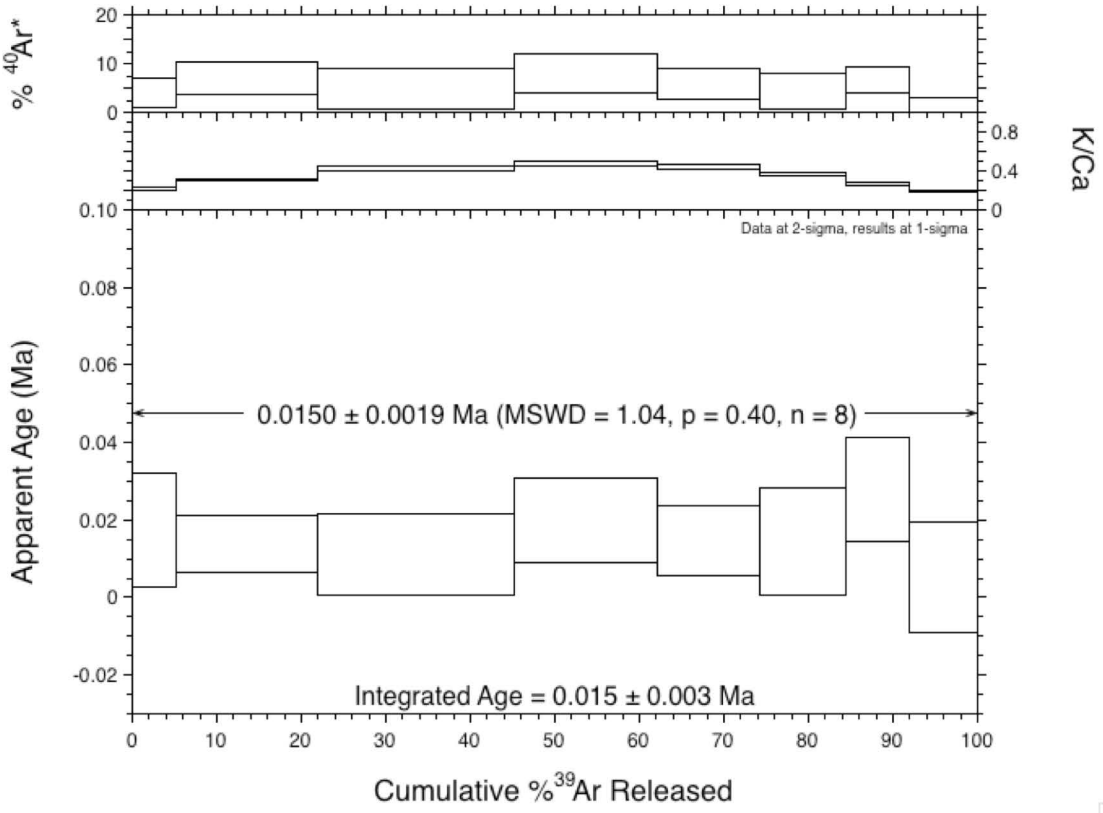
% 40Ar*
K/Ca
Data at 2-sigma, results at 1-sigma
Apparent Age (Ma)
0.0150 ± 0.0019 Ma (MSWD = 1.04, p = 0.40, n = 8)
Integrated Age = 0.015 ± 0.003 Ma
Cumulative %39Ar Released

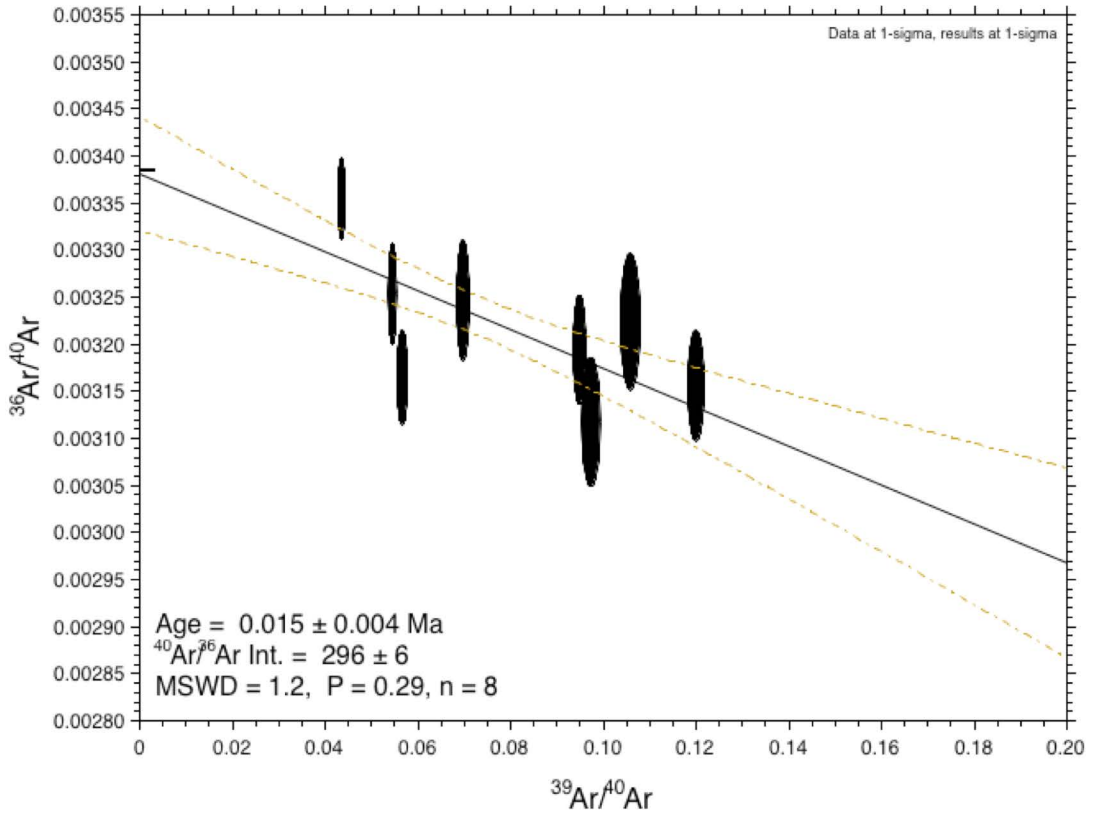
Data at 1-sigma, results at 1-sigma
36Ar/40Ar
Age = 0.015 ± 0.004 Ma
40Ar/36Ar Int. = 296 ± 6
MSWD = 1.2, P = 0.29, n = 8
39Ar/40Ar

TDCAH100

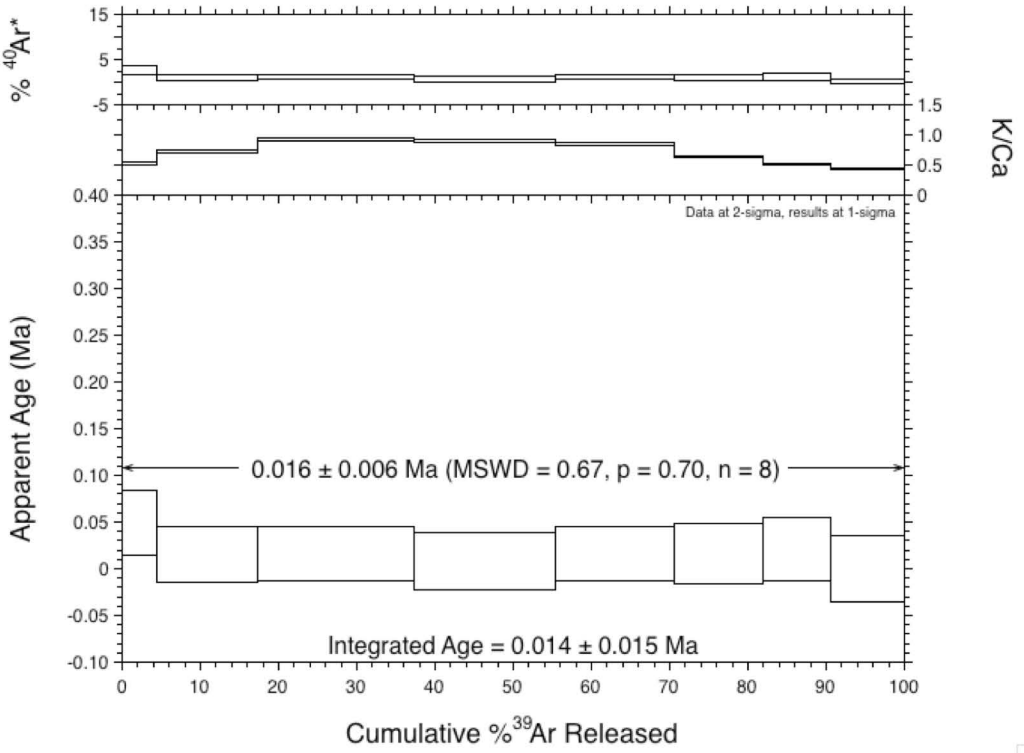
% 40Ar*
K/Ca
Data at 2-sigma, results at 1-sigma
Apparent Age (Ma)
0.016 ± 0.006 Ma (MSWD = 0.67, p = 0.70, n = 8)
Integrated Age = 0.014 ± 0.015 Ma
Cumulative %39Ar Released

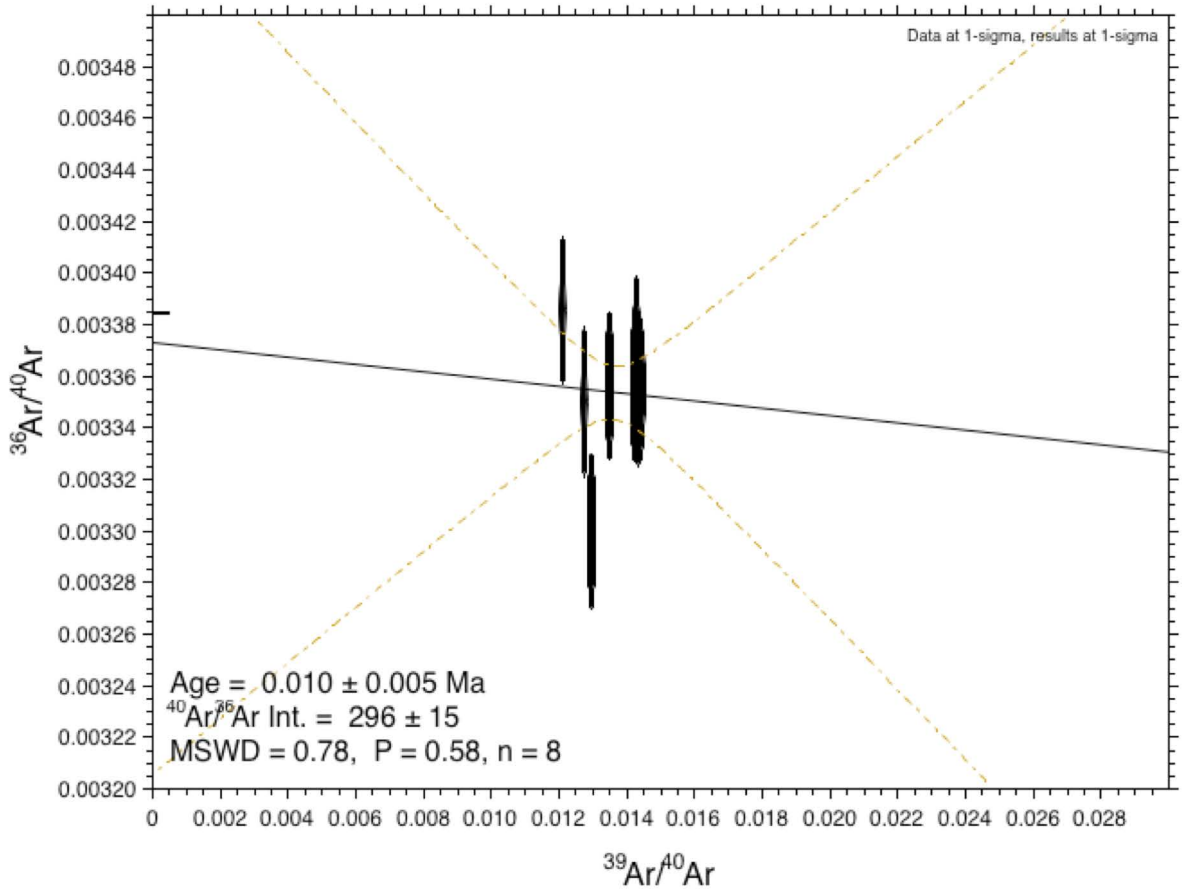
Data at 1-sigma, results at 1-sigma
36Ar/40Ar
Age = 0.010 ± 0.005 Ma
40Ar/36Ar Int. = 296 ± 15
MSWD = 0.78, P = 0.58, n = 8
39Ar/40Ar

TDCAH010

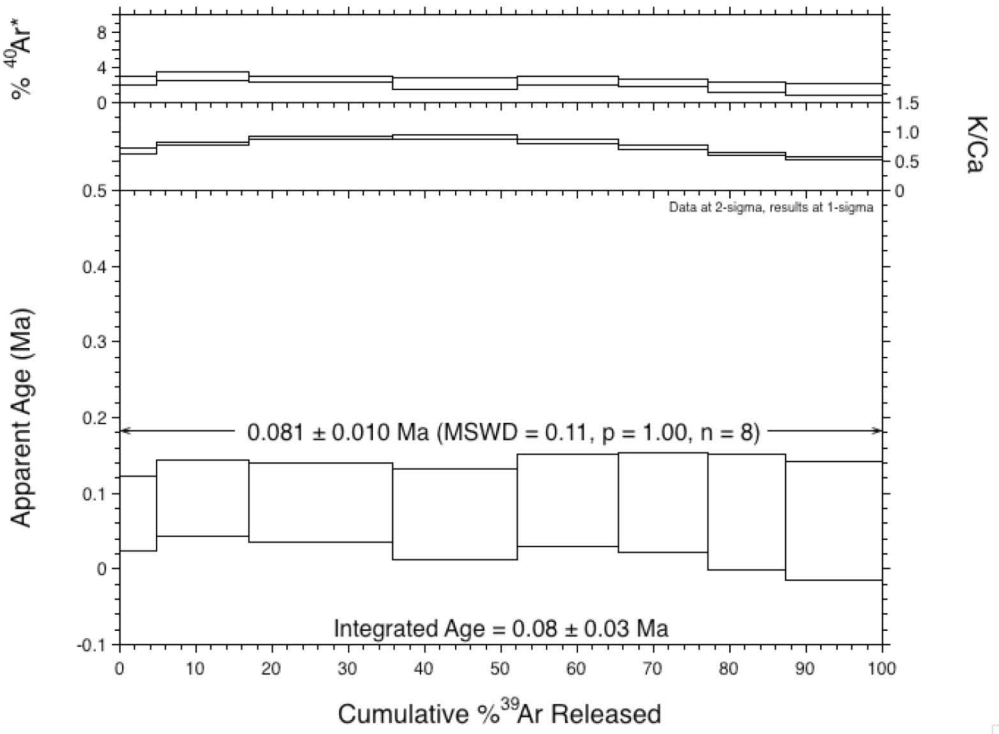
% 40Ar*
K/Ca
Data at 2-sigma, results at 1-sigma
Apparent Age (Ma)
0.081 ± 0.010 Ma (MSWD = 0.11, p = 1.00, n = 8)
Integrated Age = 0.08 ± 0.03 Ma
Cumulative %39Ar Released

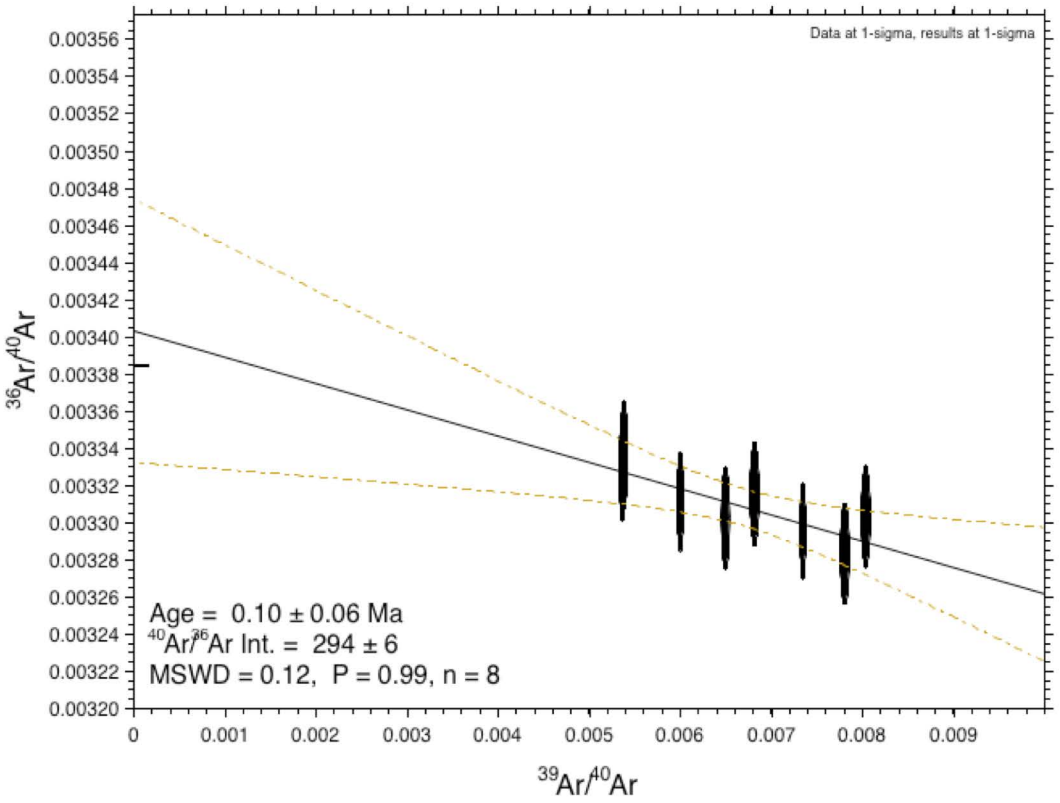
Data at 1-sigma, results at 1-sigma
36Ar/40Ar
Age = 0.10 ± 0.06 Ma
40Ar/36Ar Int. = 294 ± 6
MSWD = 0.12, P = 0.99, n = 8
39Ar/40Ar

TDCAH011

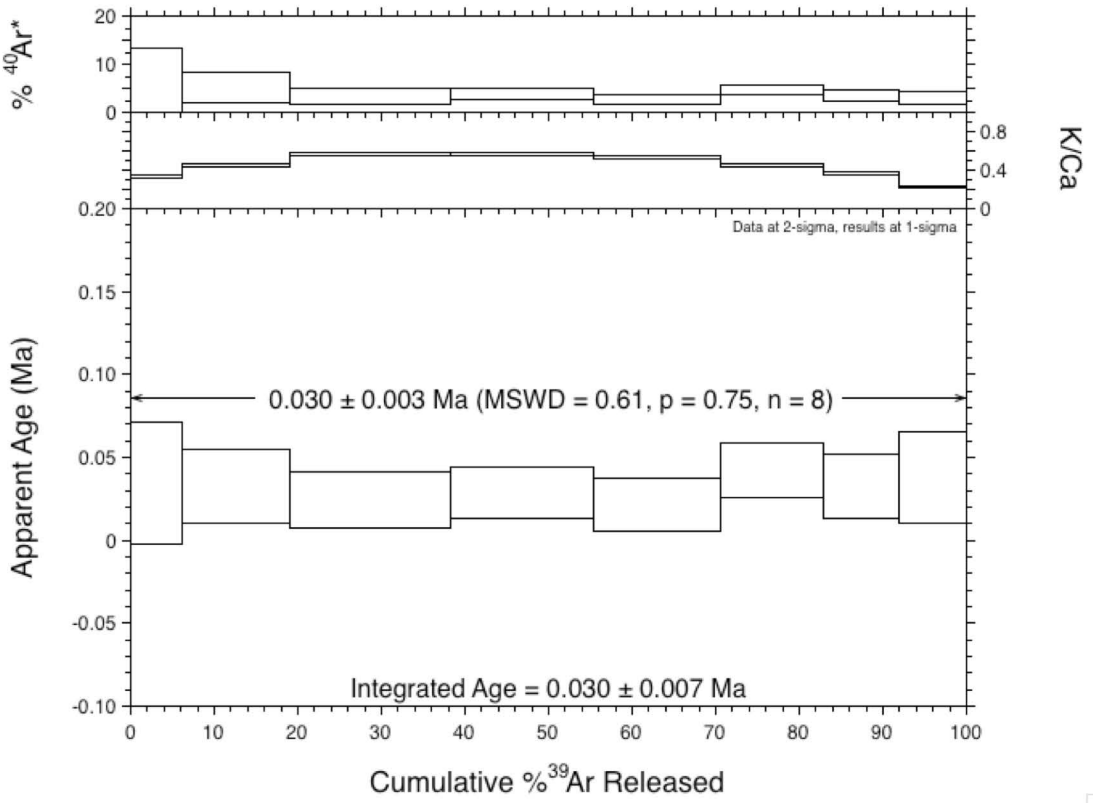
% 40Ar*
K/Ca
Data at 2-sigma, results at 1-sigma
Apparent Age (Ma)
0.030 ± 0.003 Ma (MSWD = 0.61, p = 0.75, n = 8)
Integrated Age = 0.030 ± 0.007 Ma
Cumulative %39Ar Released

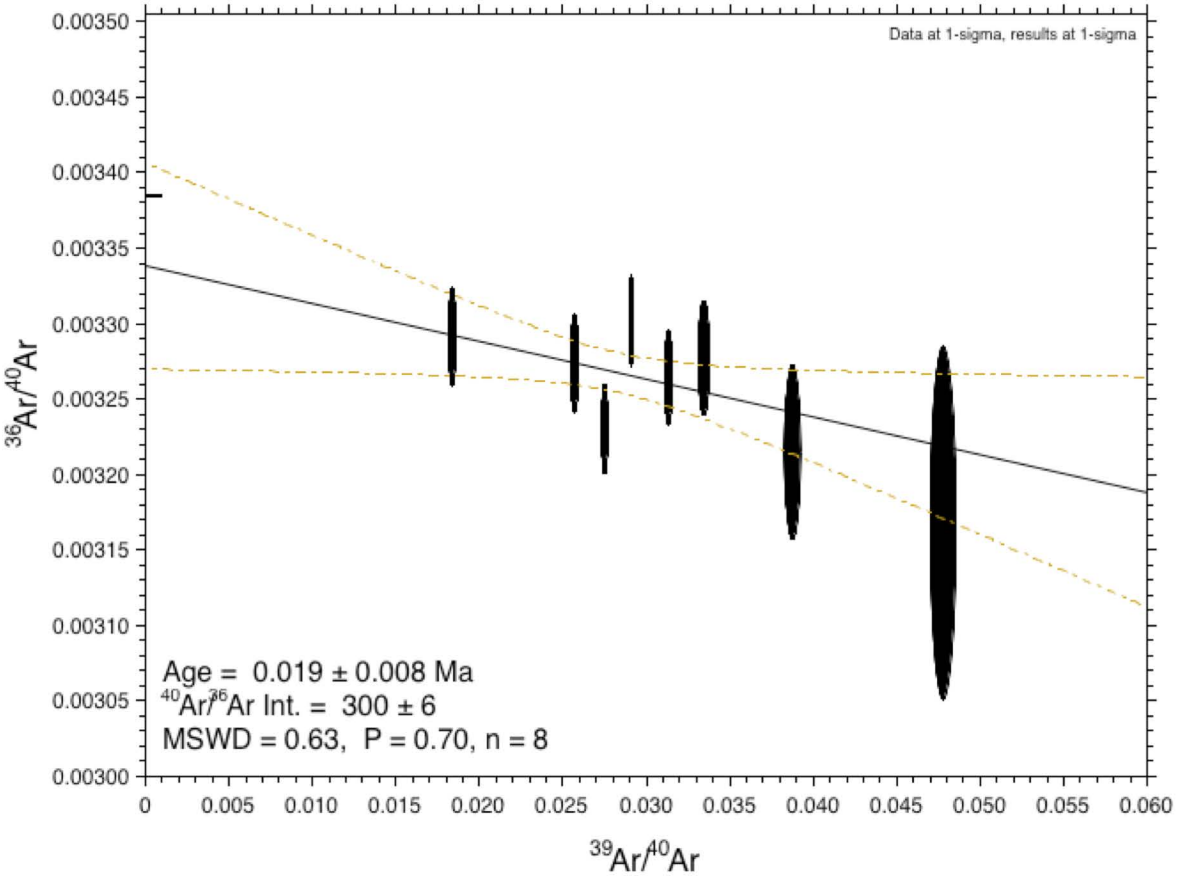
Data at 1-sigma, results at 1-sigma
36Ar/40Ar
Age = 0.019 ± 0.008 Ma
40Ar/36Ar Int. = 300 ± 6
MSWD = 0.63, P = 0.70, n = 8
39Ar/40Ar

TDCAH022

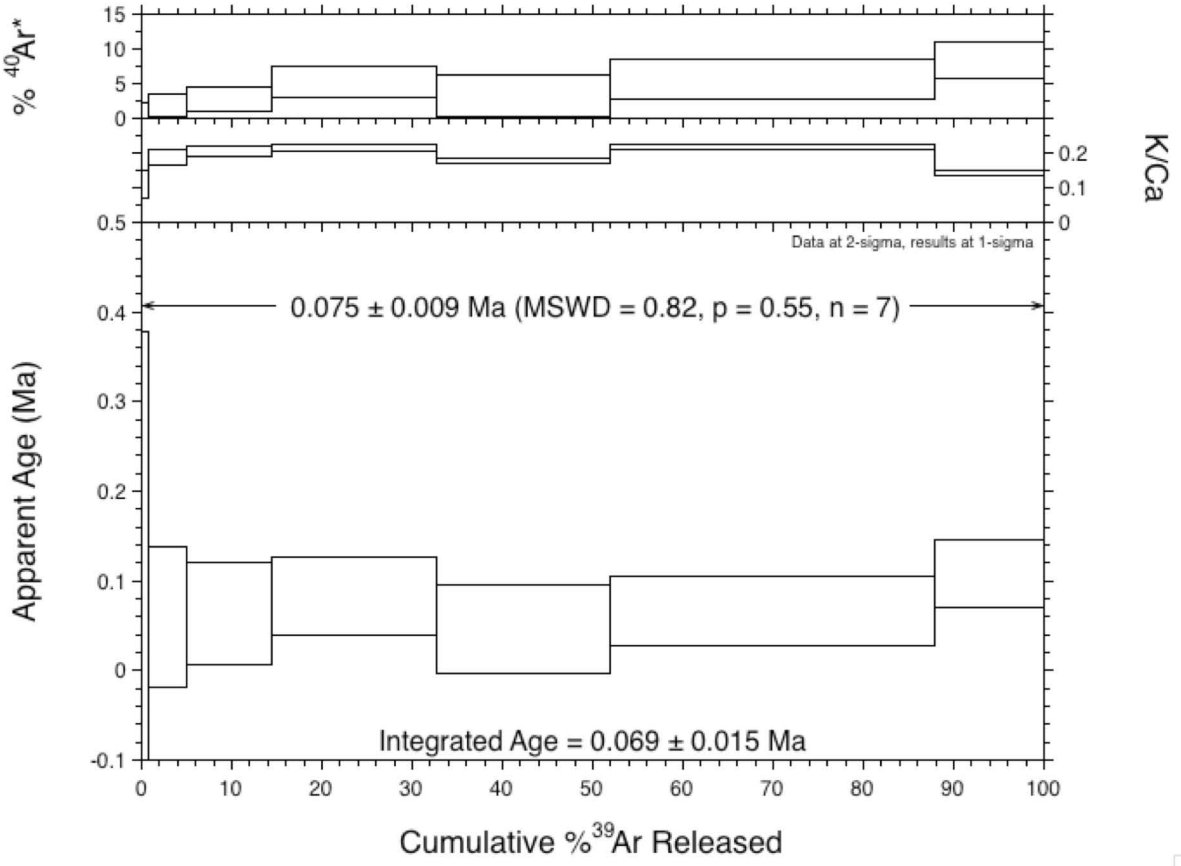
% 40Ar*
K/Ca
Data at 2-sigma, results at 1-sigma
0.075 ± 0.009 Ma (MSWD = 0.82, p = 0.55, n = 7)
Apparent Age (Ma)
Integrated Age = 0.069 ± 0.015 Ma
Cumulative %39Ar Released

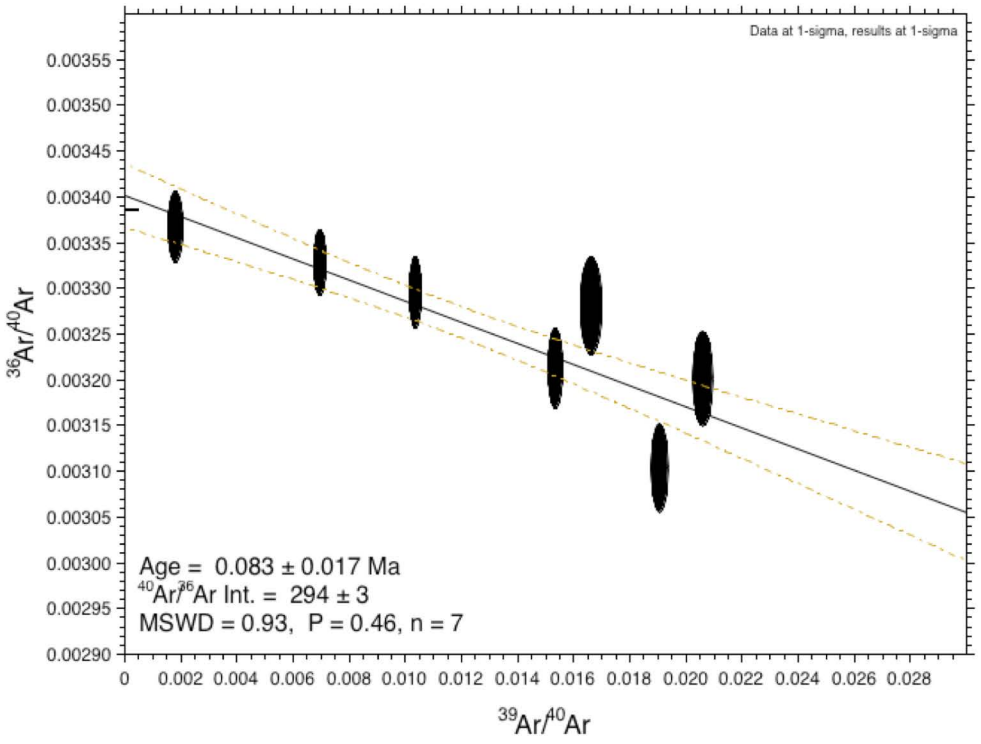
Data at 1-sigma, results at 1-sigma
36Ar/40Ar
Age = 0.083 ± 0.017 Ma
40Ar/36Ar Int. = 294 ± 3
MSWD = 0.93, P = 0.46, n = 7
39Ar/40Ar

TDCAH024

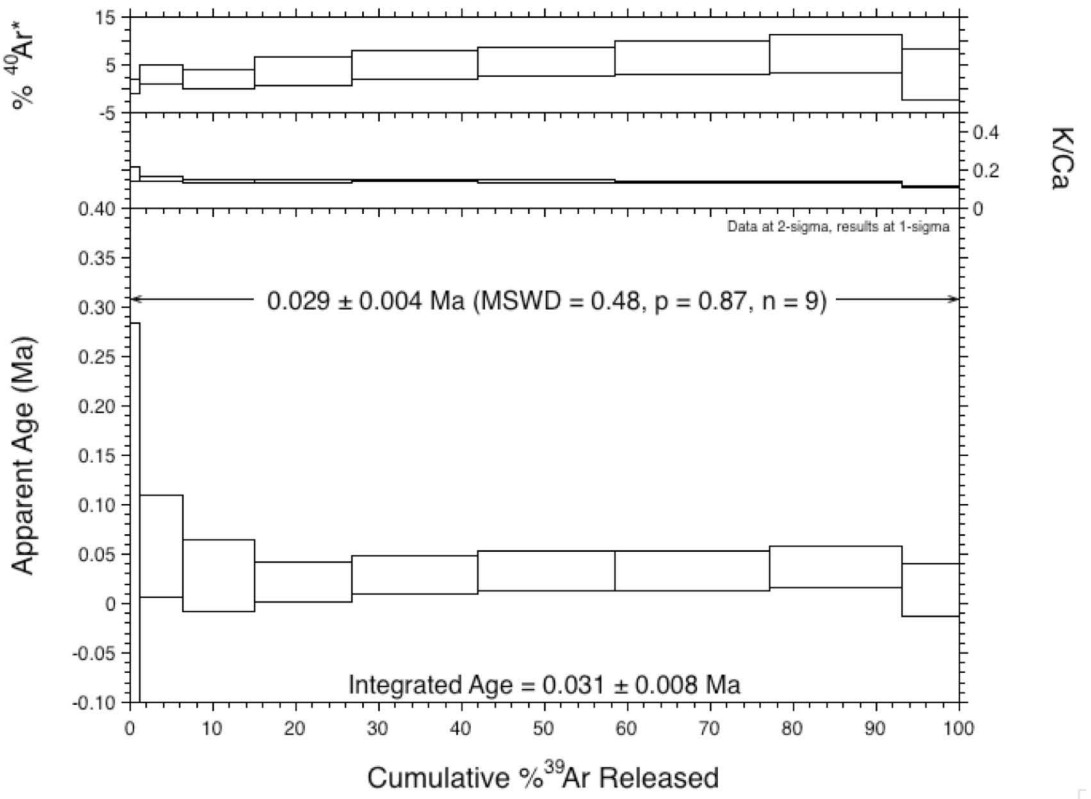
% 40Ar*
K/Ca
Data at 2-sigma, results at 1-sigma
0.029 ± 0.004 Ma (MSWD = 0.48, p = 0.87, n = 9)
Apparent Age (Ma)
Integrated Age = 0.031 ± 0.008 Ma
Cumulative %39Ar Released

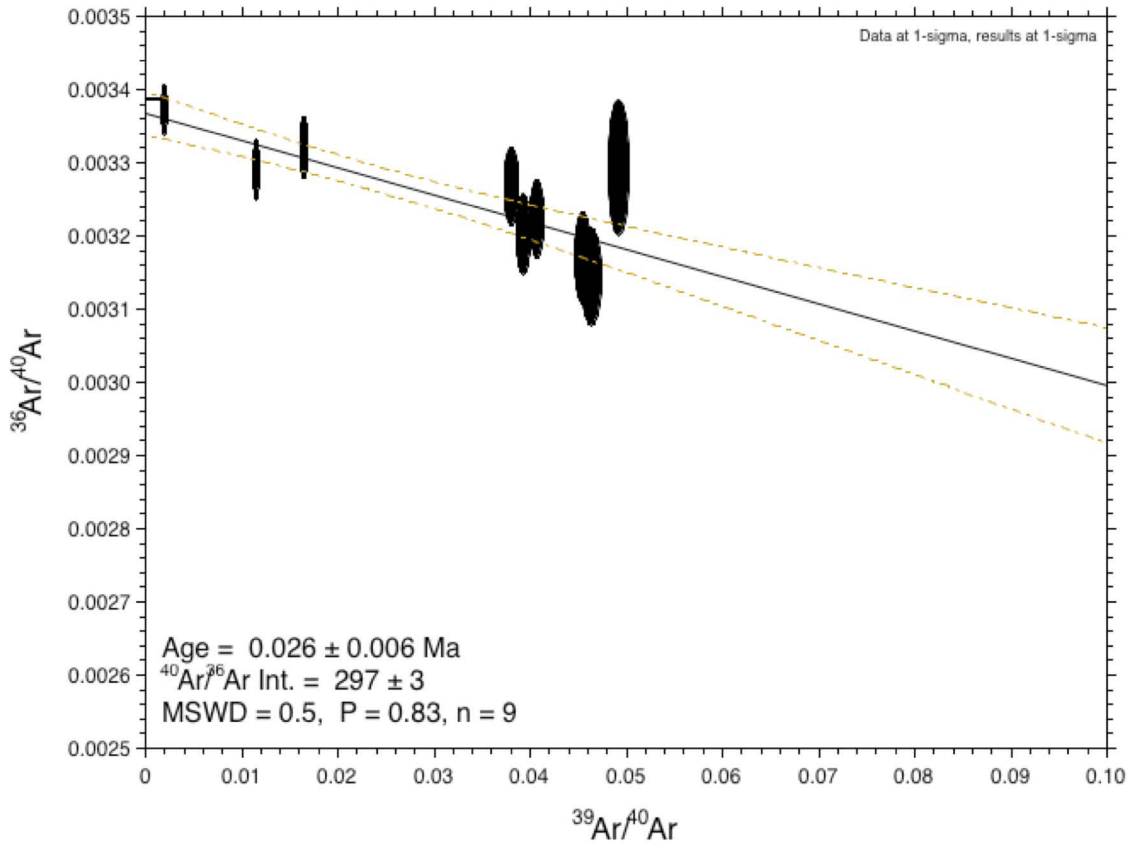
Data at 1-sigma, results at 1-sigma
Age = 0.026 ± 0.006 Ma
40Ar/36Ar Int. = 297 ± 3
MSWD = 0.5, P = 0.83, n = 9
36Ar/40Ar
39Ar/40Ar

TDCAH038

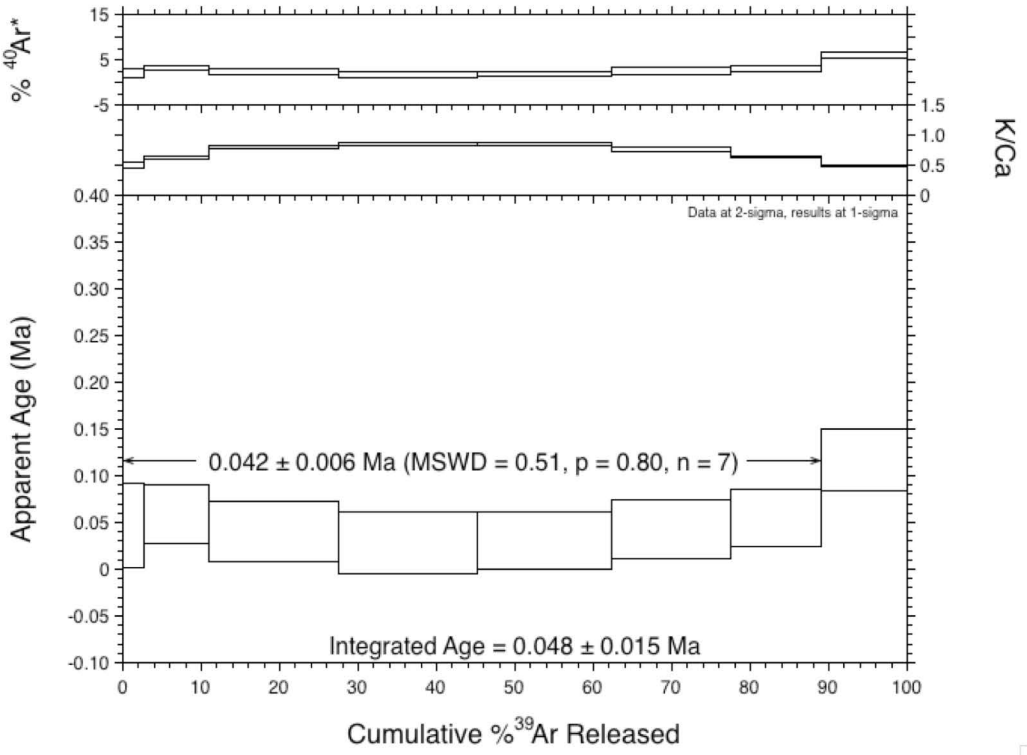
% 40Ar*
K/Ca
Data at 2-sigma, results at 1-sigma
Apparent Age (Ma)
0.042 ± 0.006 Ma (MSWD = 0.51, p = 0.80, n = 7)
Integrated Age = 0.048 ± 0.015 Ma
Cumulative %39Ar Released

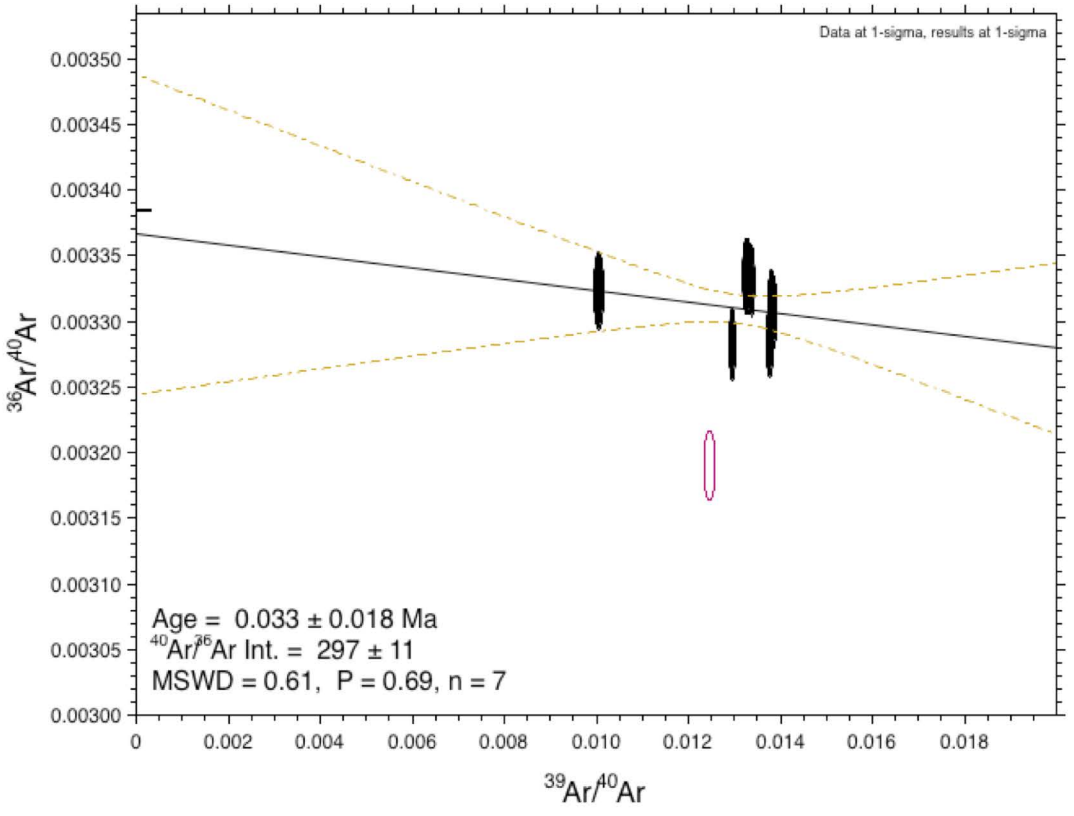
Data at 1-sigma, results at 1-sigma
36Ar/40Ar
Age = 0.033 ± 0.018 Ma
40Ar/36Ar Int. = 297 ± 11
MSWD = 0.61, P = 0.69, n = 7
39Ar/40Ar

TDCAH040

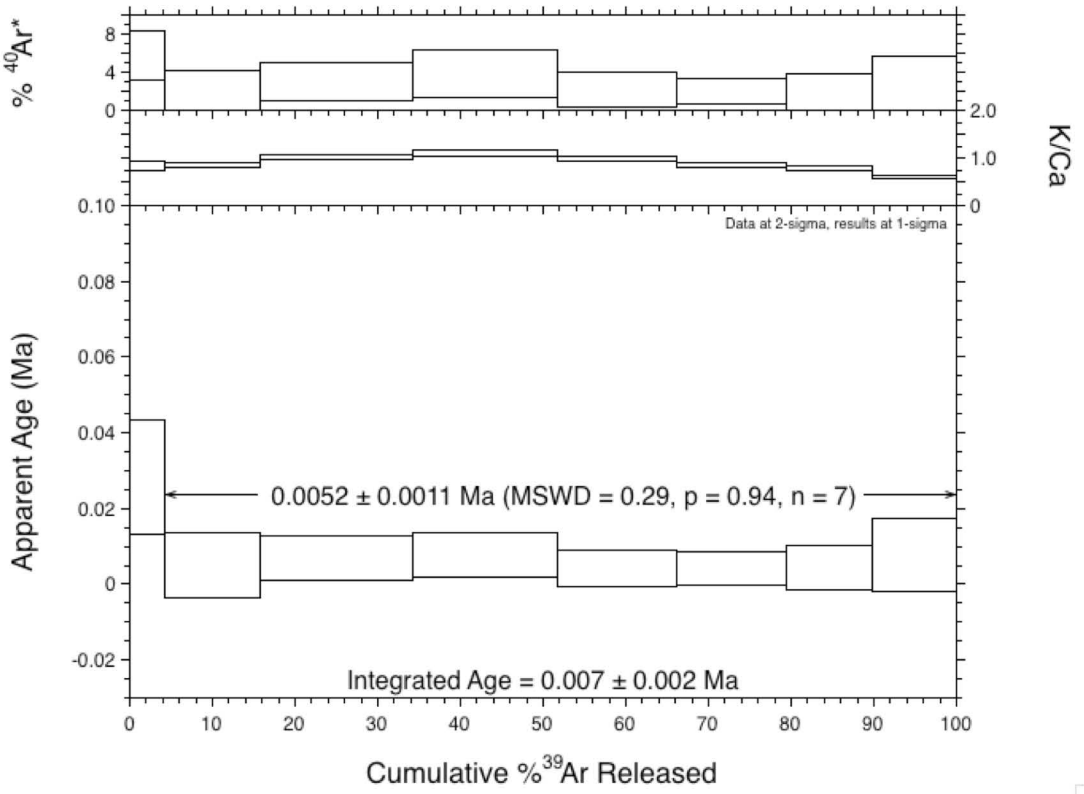
% 40Ar*
K/Ca
Data at 2-sigma, results at 1-sigma
Apparent Age (Ma)
0.0052 ± 0.0011 Ma (MSWD = 0.29, p = 0.94, n = 7)
Integrated Age = 0.007 ± 0.002 Ma
Cumulative %39Ar Released

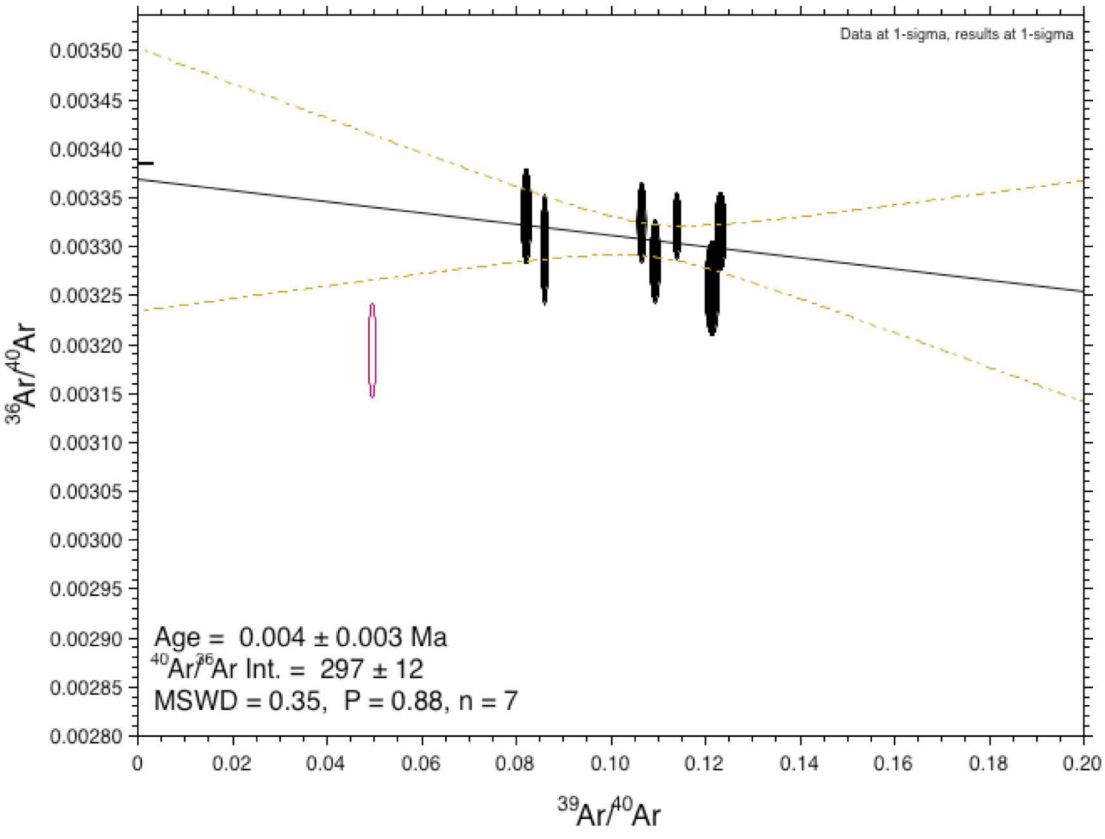
Data at 1-sigma, results at 1-sigma
36Ar/40Ar
Age = 0.004 ± 0.003 Ma
40Ar/36Ar Int. = 297 ± 12
MSWD = 0.35, P = 0.88, n = 7
39Ar/40Ar

TDCAH041

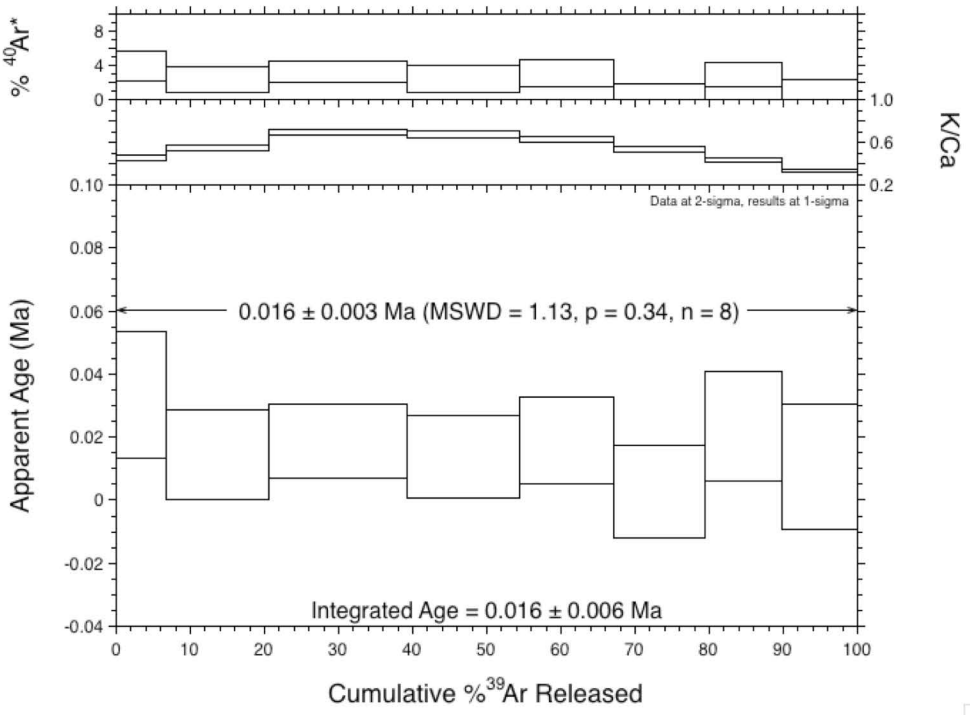
% 40Ar*
K/Ca
Data at 2-sigma, results at 1-sigma
0.016 ± 0.003 Ma (MSWD = 1.13, p = 0.34, n = 8)
Apparent Age (Ma)
Integrated Age = 0.016 ± 0.006 Ma
Cumulative %39Ar Released

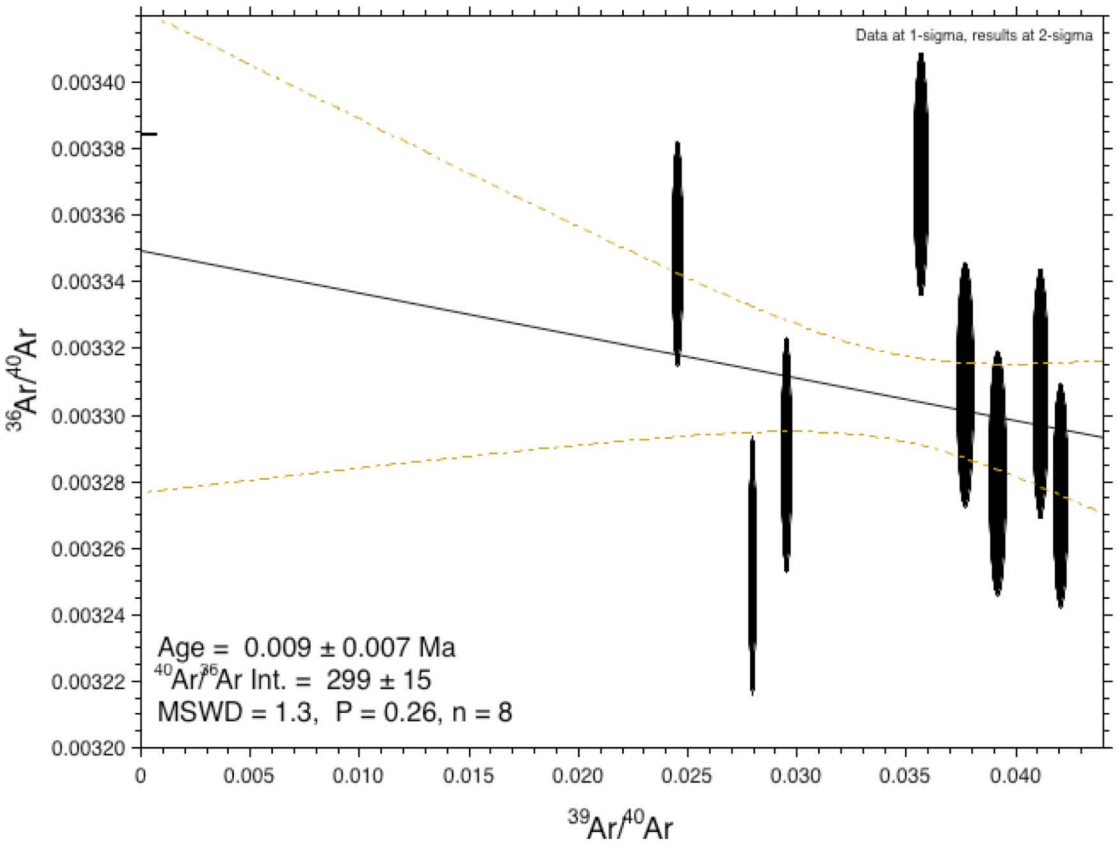
Data at 1-sigma, results at 2-sigma
Age = 0.009 ± 0.007 Ma
40Ar/36Ar Int. = 299 ± 15
MSWD = 1.3, P = 0.26, n = 8
36Ar/40Ar
39Ar/40Ar

TDCAH047

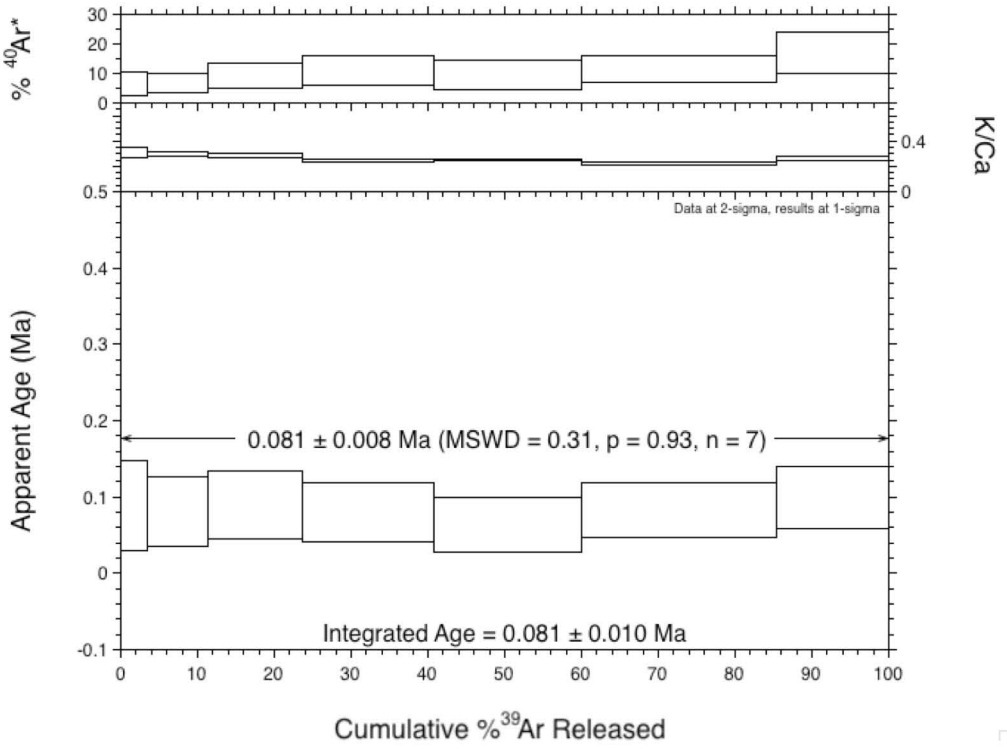
% 40Ar*
K/Ca
Data at 2-sigma, results at 1-sigma
Apparent Age (Ma)
0.081 ± 0.008 Ma (MSWD = 0.31, p = 0.93, n = 7)
Integrated Age = 0.081 ± 0.010 Ma
Cumulative %39Ar Released

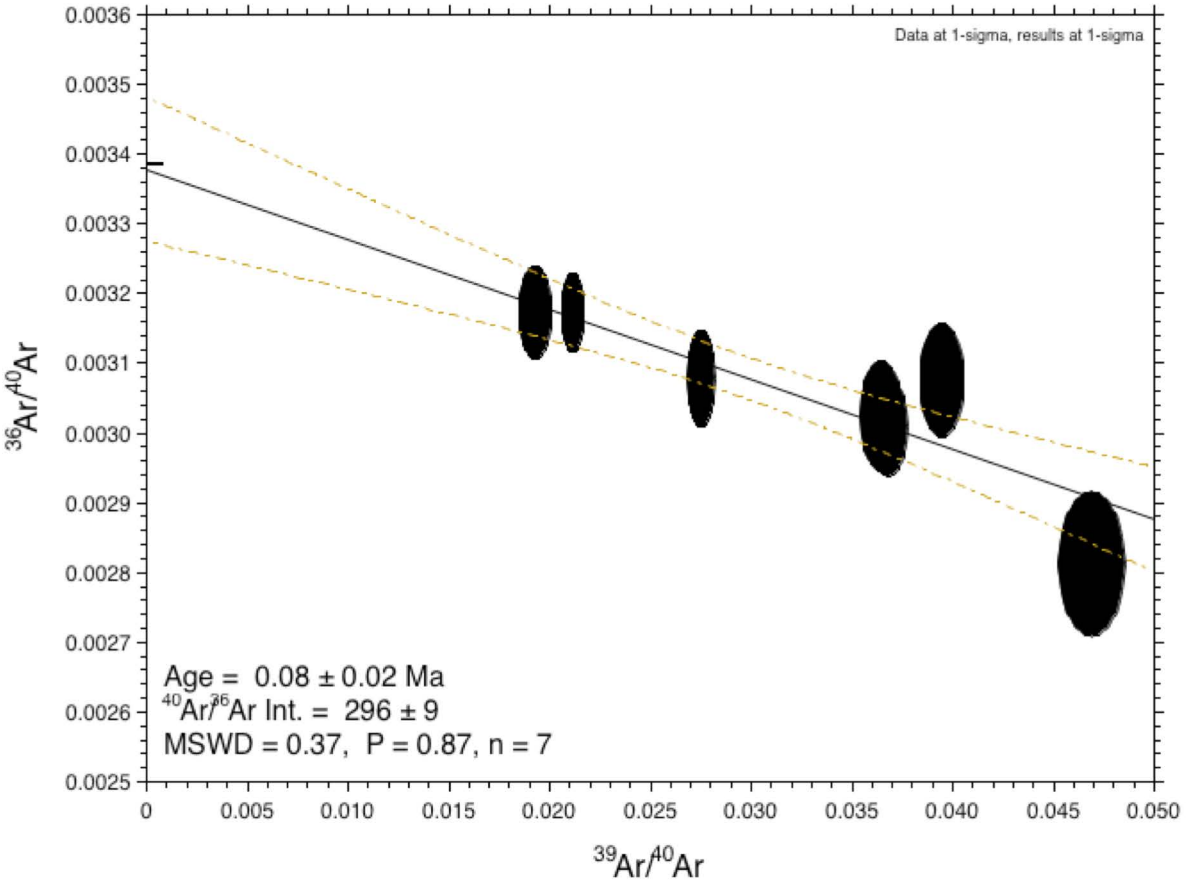
Data at 1-sigma, results at 1-sigma
36Ar/40Ar
Age = 0.08 ± 0.02 Ma
40Ar/36Ar Int. = 296 ± 9
MSWD = 0.37, P = 0.87, n = 7
39Ar/40Ar

TABLE DR1. MAJOR AND TRACE ELEMENTS FOR DATED SAMPLES

Sample number	007	010	011	022	024	038	040	041	047	052	054	085	089	093	100
MgO	4.48	4.01	4.87	4.26	1.94	0.67	2.25	5.2	2.4	4.4	4.14	4.46	3.77	6.83	4.44
Al_2O_3	16.33	17.41	15.93	16.46	18.59	20.18	19.17	15.92	18.97	17.91	17.38	16.45	17.38	14.73	16.4
SiO_2	45.98	45.65	45.02	43.09	51.78	57.27	51.84	44.49	50.05	44.68	46.04	46.08	45.91	43.02	45.4
P_2O_5	0.95	0.97	0.85	1.12	0.65	0.14	0.76	0.73	0.7	1.15	1.2	0.93	1.15	0.71	0.95
CaO	9.06	9.09	9.51	9.03	6.45	3.08	5.89	9.94	6.54	9.03	8.4	9.04	9.03	10.61	9.1
TiO_2	3.22	3.28	3.31	3.19	1.86	1.04	2.29	3.63	2.28	2.82	3.08	3.23	3.3	3.78	3.21
MnO	0.18	0.16	0.18	0.27	0.18	0.12	0.15	0.19	0.17	0.19	0.16	0.18	0.18	0.16	0.18
K_2O	3.02	2.95	1.25	2.56	2.68	5.4	4.2	2.67	3.86	2.42	3.38	3.2	1.03	0.76	3.04
Fe_2O_3	11.58	11.11	12.34	12.54	7.15	3.28	6.7	12.15	7.76	10.07	10.11	11.68	10.5	13.68	11.76
Na_2O	4.2	4.02	5.19	3.67	5.96	6	5.31	3.64	4.91	3.17	4.21	3.96	5.36	3.91	3.96
Total	99	98.65	98.45	96.19	97.24	97.18	98.56	98.56	97.64	95.84	98.1	99.21	97.61	98.19	98.41
LOI	*-0.22*	*0.18*	*0.7*	*2.42*	*1.46*	*1.74*	*1.02*	*-0.15*	*1.44*	*3.94*	*0.52*	*-0.29*	*1.18*	*0.39*	*-0.19*
Sc	12	<10	12	12	<10	<10	<10	14	<10	10	10	12	10	22	10
V	195	182	259	210	90	55	131	267	115	187	198	196	202	336	198
Cr	<20	<20	<20	<20	<20	<20	<20	<20	<20	<20	<20	<20	<20	70	<20
Ni	<10	12	<10	19	<10	<10	<10	14	<10	14	<10	<10	<10	57	<10
Cu	13	<10	16	50	<10	<10	<10	16	<10	29	<10	<10	<10	31	28
Zn	100	94	111	113	96	63	95	97	101	97	107	108	100	100	111
As	<10	<10	<10	<10	<10	<10	<10	<10	<10	<10	<10	<10	<10	<10	<10
Rb	72	68	73	56	93	155	107	70	96	55	71	73	72	49	67
Sr	1208	1264	1181	1184	1453	920	1416	1112	1365	1243	1459	1197	1442	1019	1243
Y	29	29	26	29	27	22	27	27	28	29	29	29	29	25	28
Zr	343	321	346	338	423	530	397	302	432	322	350	349	320	261	341
Nb	76	73	78	76	95	106	97	66	98	70	90	79	77	58	76
Mo	<10	<10	<10	<10	<10	<10	<10	<10	<10	<10	<10	<10	<10	<10	<10
Ba	742	725	781	720	1166	1308	1147	688	1027	818	825	726	886	555	747
La	77	74	82	84	114	99	97	70	102	77	96	73	75	60	80
Ce	196	190	205	214	256	191	219	165	228	212	226	184	214	157	191
Pb	<10	<10	<10	10	<10	13	<10	<10	<10	<10	<10	<10	<10	<10	<10
Th	11	12	13	11	15	20	15	11	16	12	13	13	11	<10	12
U	<10	<10	<10	<10	<10	<10	<10	<10	<10	<10	<10	<10	<10	<10	<10

TABLE DR3. BLANK AND MASS DISCRIMINATION DATA

Full system blanks, standard deviations taken from entire run sequence (encompassing all sample runs), *n* = 66

^{40}Ar (V)	±1s	^{39}Ar (V)	±1s	^{38}Ar (V)	±1s	^{37}Ar (V)	±1s	^{36}Ar (V)	±1s
0.009026549	0.000321	0.000274336	0.00002	0.000168142	0.000025	0.00069469	0.000019	0.000122124	0.00001

Air calibrations (monitor mass discrimination), average ± standard deviation (encompassing all sample runs), n = 21

^{40}Ar/^{36}Ar	±1s	D ^{40}Ar/^{36}Ar	D ±1s
288.3	0.6	1.0088	0.0005

NOTES:
Samples were irradiated for 5 minutes in the Cd-lined facility at McMaster. Sanidine from the Alder Creek Tuff was used as the neutron fluence monitor with a reference age of 1.193 ± 0.001 Ma (Nomade *et al.*, 2005).

Nucleogenic production ratios:

$(^{36}Ar/^{37}Ar)_{Ca}$	2.64		$\times 10^{-4}$
$(^{39}Ar/^{37}Ar)_{Ca}$	6.5		$\times 10^{-4}$
$(^{38}Ar/^{37}Ar)_{Ca}$	0.196	± 0.00816	$\times 10^{-4}$
$(^{40}Ar/^{39}Ar)_{K}$	85		$\times 10^{-4}$
$(^{38}Ar/^{39}Ar)_{K}$	1.22	± 0.0027	$\times 10^{-2}$
$(^{36}Ar/^{38}Ar)_{Cl}$	3.2		$\times 10^{2}$
$^{37}Ar/^{39}Ar$ to Ca/K	1.96		

Isotopic constants and decay rates:

$\lambda(^{40}K_{\varepsilon})$ /yr	5.81	± 0.04	$\times 10^{-11}$
$\lambda(^{40}K_{\beta^-})$ /yr	4.962	± 0.00043	$\times 10^{-10}$
$\lambda(^{37}Ar)$ /d	1.975		$\times 10^{-2}$
$\lambda(^{39}Ar)$ /d	7.068		$\times 10^{-6}$
$\lambda(^{36}Cl)$ /d	6.308		$\times 10^{-9}$
$(^{40}Ar/^{36}Ar)_{Atm}$	295.5	± 0.5	
$(^{40}Ar/^{38}Ar)_{Atm}$	1575	± 2	
$^{40}K/K_{Total}$	0.01167		